

# SELF-RESTRICTING NOISE AND QUANTUM RELATIVE ENTROPY DECAY

NICHOLAS LARACUENTE

ABSTRACT. Open quantum systems as modeled by quantum channels and quantum Markov semigroups usually decay to subspaces that are invariant under environmental interactions. It is known that finite-dimensional semigroups with detailed balance decay exponentially under modified logarithmic-Sobolev inequalities (MLSIs). Here we analyze discrete and continuous processes that include unitary components, breaking the detailed balance assumption. We find counter-examples to analogs of MLSIs for these systems. The generalized quantum Zeno effect appears for many Lindbladians that combine a decay process with unitary drift. As incompatible long-time and Zeno limits compete, strong noise often protects subsystems and subspaces from its own spread. We observe this interplay between decay and Zeno-like effects experimentally on superconducting qubits using IBM Q devices. Nonetheless, by combining MLSIs for effective self-adjoint decay processes across different times, we obtain eventual exponential decay. We similarly obtain decay rate lower bounds for discrete compositions of quantum channels.

## 1. INTRODUCTION

A quantum state exposed to a stationary environment usually decays toward a state that is invariant under environmental interactions. This open time-evolution is responsible for decoherence, the equilibration of thermal systems, the capability to non-unitarily reset a qubit mid-computation, and many other essential processes in quantum information.

A (Schrödinger picture) Lindbladian generator  $\mathcal{L}$  generates a quantum Markov semigroup  $\Phi^t(\rho) = \exp(-\mathcal{L}t)(\rho)$  [Lin76, GKS76]. The Lindbladian is an open system generalization of the Hamiltonian to non-unitary dynamics. Quantum Markov semigroups can induce non-invertible processes, as information is lost to the environment.

In contrast to Hamiltonians are Lindbladians that have detailed balance, a property related to time reversal symmetry [CM17]. Recently, a series of results [JLR19, GJL21, GR21] confirmed that all Lindbladians having detailed balance with respect to a GNS inner product obey a *complete, modified logarithmic-Sobolev inequality* (CMLSI) based on the modified logarithmic Sobolev inequality defined in [AMTU98, BT03, KT13]. For a semigroup  $(\Phi^t : t \in \mathbb{R}^+)$  in terms of the quantum relative entropy  $D(\cdot\|\cdot)$ ,  $\lambda$ -CMLSI states that

$$D(\Phi^t(\rho)\|\mathcal{E}(\rho)) \leq e^{-\lambda t} D(\rho\|\mathcal{E}(\rho)), \quad (1)$$

where  $\lambda > 0$ , and  $\mathcal{E}$  is a projection to the invariant or fixed point subspace of  $\Phi^t$ . Furthermore, the “completeness” of the inequality refers to its stability under tensor extensions and products:

---

NL is supported by IBM as a Postdoctoral Scholar at the University of Chicago & the Chicago Quantum Exchange.

we may extend  $\Phi^t$  to  $\Phi^t \otimes \text{Id}^n$  for an auxiliary system of any size  $n$ , and the CMLSI constant  $\lambda$  remains the same.

Nonetheless, important questions remained open. In particular, the presence of a Hamiltonian generator precludes detailed balance, so should CMLSI still hold? We consider (adjoint) Lindbladian generators <sup>1</sup> of the form

$$\mathcal{L}(\rho) = i[H, \rho] + \mathcal{S}(\rho), \quad (2)$$

where  $\mathcal{S}$  is a Lindbladian with GNS detailed balance, and  $H$  is a Hamiltonian generator of unitary time evolution. The semigroup  $\Phi^t$  arises as  $\Phi^t = \exp(-t\mathcal{L})$ . Let  $\mathcal{E}_0 := \lim_{t \rightarrow \infty} \exp(-t\mathcal{S})$  denote the fixed point conditional expectation of  $\mathcal{S}$ . We may refer to  $H$  as generating coherent dynamics, rotation, or drift, and to  $\mathcal{S}$  as generating stochastic dynamics or decay. We refer to this form as a decay+drift Lindbladian.

Decay+drift Lindbladians commonly induce generalized Zeno-like effects. Historically, the quantum Zeno effect is usually stated as frequent measurements suppressing the time-evolution of a quantum system away from the basis of measurement [MS77]. A number of results that include versions of the generalized Zeno effect [BZ18, MW19, BFN<sup>+</sup>20, BDS21, MR21], dynamical decoupling [FLP04, HBY21], and adiabatic theorems [Kat50, BFN<sup>+</sup>19] show that in general, a quantum process that rapidly changes the state will modify the effective dynamics of a simultaneous, slower process. Frequent applications of a channel or a continuous process with detailed balance may suppress dynamics of a concurrent Hamiltonian. As a consequence (Theorem 3.4), we show that a Lindbladian in the form Equation (2) admits an upper bound on overall decay rate that is inverse to  $\mathcal{S}$ 's CMLSI constant when  $\mathcal{S}$  has sufficiently fast CMLSI.

Analogous to CMLSI, we define a notion of rotated CMLSI with a time-varying, decay-invariant subspace. While this notion extends the concept of CMLSI beyond the detailed balance setting, we find that it does not hold in general. Some systems decay sub-exponentially at short times as demonstrated in Counterexamples 3.1 and 3.2. Intuitively, when a system undergoes decay and drift simultaneously, one may view the drift in a Heisenberg-inspired picture as time-evolving the decay process. The initial decay might not be representative of its eventual effects. In these scenarios, information may hide in a subsystem or basis that will eventually rotate into a more noise-affected position. More broadly, strong noise induces a competition between Zeno-like effects and long-time decay. In the limit of overwhelming noise, the overall decay rate of the decay+drift Lindbladian decreases with increasing strength of the stochastic part.

## 2. EXPERIMENTAL AND NUMERICAL RESULTS

**2.1. Simulated Spin Chain with Depolarizing Endpoint.** To illustrate the observed phenomena, we start by considering a simple, commonly studied physical system: a spin chain in one spatial dimension with open boundary conditions. Using Qiskit Dynamics, we consider the

---

<sup>1</sup>Conventionally in mathematics, the Lindbladian would be a Heisenberg picture operator on observables, and we would study its predual under the GNS inner product with respect to the trace,  $\mathcal{L}_*$ . Since we almost entirely work with the Schrödinger picture superoperator as acting on densities, we denote this by  $\mathcal{L}$  instead of  $\mathcal{L}_*$  and its Heisenberg picture dual by  $\mathcal{L}^*$ .

same  $XX + YY$  nearest neighbor interaction (see [noa21] for a simple example of a similar system). We add depolarizing noise to the first qubit in the chain, which continuously randomizes the state of that subsystem concurrently with the aforementioned interactions. The simulated Lindbladian has the form

$$\mathcal{L} = -2\pi i \sum_{j=1}^3 (X_j X_{j+1} + Y_j Y_{j+1}) + \gamma (\hat{1}/2 \otimes \rho^B - \rho). \quad (3)$$

We simulate and compute relative entropy of the 4-qubit chain with respect to its fixed point of complete mixture, starting from initial state  $|0000\rangle$  or  $(\hat{1}/2)^{\otimes 3} \otimes |0\rangle\langle 0|$ . Results are plotted in Figure 1.(1). We denote by  $\gamma$  a parameter multiplying the noise terms, which controls the strength of noise relative to time and interaction terms.

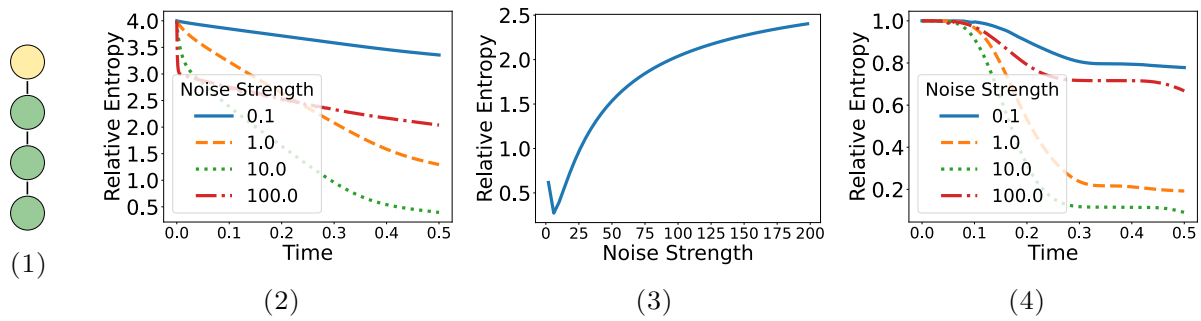


FIGURE 1. Relative entropy of a 4-qubit spin chain to complete mixture: (1) Illustration of the spin chain. The noised qubit is on top and shaded yellow. The 3 qubits below are shaded green with nearest-neighbor interactions. (2) Relative entropy vs. time for simulated spin chain with input  $|0000\rangle$ , where the legend notes  $\gamma$  in Equation (3); (3) Relative Entropy vs.  $\gamma$  at time  $t = 0.5$  with input  $|0000\rangle$ ; (4) Relative entropy vs. time with input  $(\hat{1}/2)^{\otimes 3} \otimes |0\rangle\langle 0|$ .

Figure 1.(1) initially shows faster relative entropy decay with larger  $\gamma$  as expected, but this pattern soon breaks. We observe that  $\gamma$  is strongly and directly correlated with the slope of the initial relative entropy decay until the entropy reaches 1 bit. This point corresponds to nearly complete mixing of the noised qubit. After this point, the spread of noise is primarily limited by interactions, so it is not surprising that large increases in the noise strength have a less substantial effect on later parts of the curve. What's more surprising is the apparent inversion in the relationship between noise strength and entropy decay when going from 10.0 to 100.0. Figure 1.(2) further illuminates this observation by showing relative entropy at fixed time as a function of  $\gamma$ . While decay rate expectedly correlates with noise strength for weak noise, the relationship soon inverts. Counter-intuitively, strong noise slows decay. The resolution to this oddity turns out to be a Zeno-like effect known as the generalized adiabatic theorem [BFN<sup>+</sup>19]. Extremely strong noise actually suppresses the interaction between the noised qubit and the others, slowing its own spread.

In Figure 1.(3), we examine the same model with initial state  $(\hat{1}/2)^{\otimes 3} \otimes |0\rangle\langle 0|$  at an enlarged range of noise scales. Here we see almost no initial decay, and as suspected, this case will form the base of Counterexample C.6 to general CMLSI. Since the short-time decay is too slow, this system does not have CMLSI. The intuition for this phenomenon is that since the three qubits closest to the noise are already completely mixed, it takes some time for the pure part of the state to propagate to where it is substantially exposed to noise. In the Heisenberg picture, the noise must propagate to the end of the chain that is not already in an invariant subspace.

This simple example serves primarily to motivate the further studies in this paper. First, however, we turn to an even simpler system to study experimentally.

**2.2. Self-Restricting Noise in a 2-Qubit Interaction.** Consider the following scenario: two qubits  $A$  and  $B$  undergo coherent time-evolution under an interaction Hamiltonian  $H = Z \otimes X/2$ , while  $A$  undergoes depolarizing noise. Hence the system’s evolution is described by the (adjoint) Lindbladian

$$\mathcal{L}(\rho) := -i[Z \otimes X/2, \rho] + \gamma(\hat{1}/2 \otimes \rho^B - \rho). \quad (4)$$

The fixed point conditional expectation of the stochastic part,  $\mathcal{S}(\rho) = \gamma(\hat{1}/2 \otimes \rho^B - \rho)$ , is  $\mathcal{E}_0(\rho) = \hat{1}/2 \otimes \rho^B$ . Here  $\mathcal{E}_0(H) = 0$ , yielding a generator of the identity. Let  $\Phi_{ZX(t)}$  denote the unitary generated by  $H$  in time  $t$ .

**2.2.1. Simulations Approaching Continuum.** We simulate time-evolution under  $\mathcal{L}$  using Qiskit. We first choose  $t = 4\pi$  so that a fully coherent rotation results in perfect fidelity with the original state. We choose an input state of  $|00\rangle\langle 00|$ , which decays to complete mixture. We vary  $\gamma$  such that  $(1 - \exp(-\gamma t))$  (the depolarizing likelihood) falls between  $3.35 * 10^{-8}$  and 1.0, scaled logarithmically. Since qubit  $A$  is assumed fully depolarized, we study how qubit  $B$  decays away from its initial state and toward the expected fixed point of complete mixture. Results appear in Figure 2.

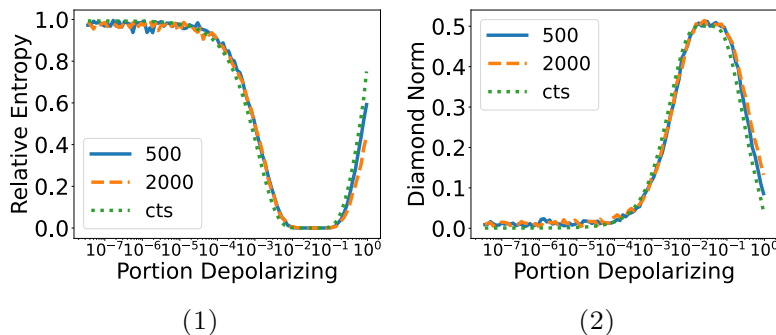


FIGURE 2. Plots of metrics for simulated noise on qubit  $B$ . Legend shows the value of the step number in a Trotter decomposition or “cts” when the simulation is for continuous time in Qiskit Dynamics. (1) Relative entropy to the fixed point under dephasing, which for this input is completely mixed. (2) Diamond norm distance to the original state.

We observe counter-intuitively non-monotonic decay with noise strength. For very small values of  $\gamma$ , the state expectedly does not decay noticeably. As we tune  $\gamma$  up, we see a region of strong decay, where a time of  $4\pi$  is long enough to mostly dephase qubit  $B$  under almost continuous interactions with a regularly noised qubit  $A$ . With large  $\gamma$ , however, the relationship inverts. As the noise channel approaches completely depolarizing, we see the decay slow with increasing  $\gamma$ . We also see that the results are not strongly dependent on the Trotter step number.

*2.2.2. Discrete Zeno-Like Effect in Experiment.* To better understand and confirm observations from Subsubsection 2.2.1, we recall the analogy between the generalized Zeno effect [MW19, BFN<sup>+</sup>20], which describes continuous processes frequently interrupted by discrete channels, and the adiabatic Theorem [BFN<sup>+</sup>19], in which a fast, continuous process suppresses some aspects of a simultaneous, slower, continuous process. In this Section, we experimentally observe the generalized Zeno effect for depolarizing noise.

Since a rotation of  $\pi/2$  corresponds to a fully entangling gate, we take  $t = \pi/2$  to maximize the potential effect of interruptions. We consider the channel given by

$$\Phi_{(k)} = (\mathcal{E}_0 \circ \Phi_{ZX(\pi/(2k))})^k \circ \mathcal{E}_0. \tag{5}$$

The total time is constant at  $\pi/2$ , but the number of interruptions is  $k$ . Combining Equation (4) with a Zeno-like bound derived from Proposition B.5 in the Supplementary Information, a tightened special case of Theorem 3.3, we calculate theoretically that

$$\|\Phi_{(k)} - \mathcal{E}_0\|_{\diamond} \leq \min \left\{ \frac{\pi^2}{8k} e^{\pi/2k}, 1.0 \right\}. \tag{6}$$

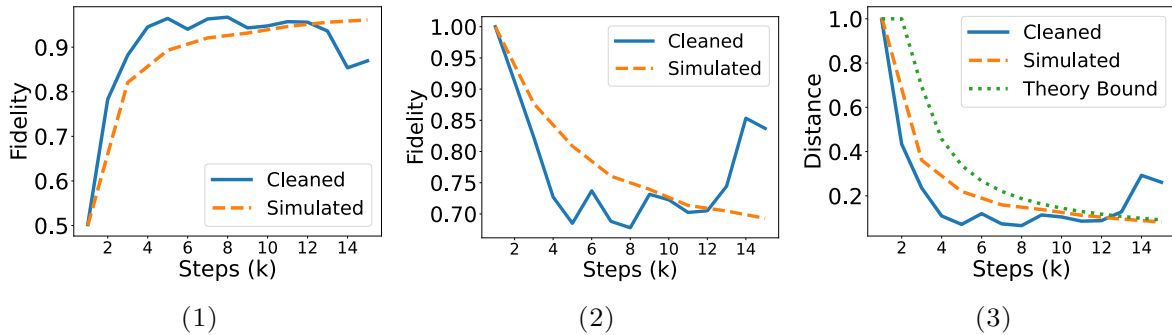


FIGURE 3. Plots of metrics for qubit  $B$  undergoing the channel described by Equation (5) via de-noised data. (1) Process fidelity of channel with identity. (2) Process fidelity with the long-time fixed point. (3) Diamond norm distance from the Zeno limit with theoretical bound from Equation (6).

We implement  $\Phi_{(k)}$  experimentally on IBM Q system as described in Subsection 5.1. Overall, we observe the expected generalized Zeno dynamics: as  $k$  increases, qubit  $B$  is protected from interactions with the frequently depolarized qubit  $A$ . The real experiment appears to converge to Zeno dynamics more quickly than its simulated, noiseless counterpart, as seen in Figures 3.(1)

and 3.(3). The accelerated convergence is potentially explainable by a small but  $k$ -independent under-rotation in each instance of  $\Phi_{ZX(t)}$ , which compounds with increasing  $k$ .

Comparing the experimental results shown in Figure 3 to theory and simulation, we first see qualitative agreement. Since 6 is intended as an upper bound, not a prediction of the experimental value, we do not necessarily expect quantitative agreement. We calculate that the simulated values of diamond norm distance to the Zeno limit as in Figure 3.(3) are on average within 20% the theoretical bound and the experimental values on average within 66%. We do see that the experimental value exceeds the ideal upper bound at large step times, which probably reflects the prevalence of realistic noise that is not part of the model.

### 3. THEORETICAL RESULTS

In this Section, we theoretically explain and generalize the preceding observations. We would in principle aim to replay the CMLSI program with rotation. We will instead discover several barriers, some simply technical and others more fundamental.

The addition of rotation to the fixed point projector largely accounts for a technical complication: unitary components in a semigroup may continue to rotate states within protected subspaces indefinitely, so they need not have a projector to an invariant subspace. Purely Hamiltonian time-evolution is the simplest possible example of a non-trivial semigroup that never decays to a fixed point. To accommodate this and more sophisticated examples, we introduce a rotated analog of (C)MLSI denoted (C)RMLSI (for rotated MLSI). We say that a semigroup has RMLSI if it converges in relative entropy to  $R_t\mathcal{E}$ , where  $\mathcal{E}$  is a projector and  $\mathcal{R}_t$  a time-dependent unitary rotation commuting with that projector. The complete version, CRMLSI, is defined analogously on arbitrary extensions by an auxiliary system. Similarly, we say that a quantum channel  $\Phi$  has  $\lambda$ -decay if  $D(\Phi(\rho)\|R\mathcal{E}(\rho)) \leq D(\rho\|\mathcal{E}(\rho))$  for some rotation  $R$ . (C)RMLSI is formally defined in Definition 5.2 and its discrete-time analog in Definition 5.1. In Equation (2), if  $\mathcal{E}_0$  and  $H$  commute, we can decouple these effects and find that  $\mathcal{L}$  has RMLSI with the same constant that  $\mathcal{S}$  has MLSI (see Proposition C.5 in the Supplementary Information).

The detailed balance condition states that for any pair of operators  $x, y$ ,  $\text{tr}(\omega x^\dagger \mathcal{L}(y)) = \text{tr}(\omega \mathcal{L}(x)^\dagger y)$ , where  $\dagger$  denotes Hermitian conjugation. This condition is a self-adjointness with respect to the  $\omega$ -weighted GNS inner product, as described in Subsection 5.1. General unitary rotations are not compatible with this self-adjointness condition. Unlike the detailed balance case, in which universal CMLSI holds across all finite-dimensional scenarios, RMLSI yields a more complicated story.

**3.1. Barriers to Decay.** RMLSI does not hold for all finite-dimensional semigroups, as illustrated by the following counterexamples.

**Counterexample 3.1** (Nearest-Neighbor Interactions with Endpoint Noise). In this counterexample, we consider an  $n$ -qubit Hamiltonian of the form  $H = \sum_{j=1}^n H_{j,j+1} + H_j$ . This form represents nearest-neighbor interactions on a one-dimensional chain with open boundary conditions. Notable examples include the Heisenberg and Ising models. We also consider a stochastic generator  $\mathcal{S} = \mathcal{S}_1 \otimes \hat{1}^{\otimes n-1}$ , which acts only on the leftmost qubit. Physically, we may think of

such a system as well-isolated except for the left end of the chain. Until the  $(n - 1)$ th term in a Taylor expansion of the semigroup around  $t = 0$ , no term contains more than  $n - 2$  qubit swaps.

Via continuity of relative entropy to a subalgebra restriction (see [Win16, Lemma 7] and [GJL20b, Proposition 3.7]),

$$D(\Phi^t(\rho)\|\mathcal{E}(\rho)) \geq (1 - O(t^{n-1} \log t))D(\rho\|\mathcal{E}(\rho)) .$$

Since  $\Phi^t$  cannot have RMLSI with any  $\lambda > 0$ , it does not have RMLSI.

To be more specific, consider a swap chain in which  $H = (n - 1)\hat{1} + \sum_{j=1}^{n-1} X_j X_{j+1} + Y_j Y_{j+1}$  as in Subsubsection 2.1. Let  $A_1, \dots, A_n$  denote qubit subsystems. We add a stochastic generator of noise on the 1st qubit,  $\mathcal{S}(\rho) = \rho - \hat{1}/2 \otimes \text{tr}_{A_1}(\rho)$ . The equilibrium state of the swap chain is an overall complete mixture. Now consider the input state  $\rho = (\hat{1}/2)^{\otimes(n-1)} \otimes |0\rangle\langle 0|$ , which is in equilibrium everywhere except the rightmost qubit. Even if the pure qubit were continually moving to the left with no possibility of reversing, we would expect it to take  $\Omega(n - 1)$  steps to reach the left end and undergo noise. Correspondingly, relative entropy decay at small  $t$  proceeds as  $O(t^{n-1} \log t)$ , representing sublinear tunneling amplitude for the state at one end to undergo noise at the other. This counterexample is illustrated numerically in Subsubsection 2.1.

**Counterexample 3.2** (Dephasing + Basis Drift). Consider the Lindbladian

$$-\mathcal{L}(\rho) = -i[X, \rho] + \gamma(Z\rho Z - \rho) ,$$

where  $X, Z$  are the usual qubit Pauli matrices. This Lindbladian combines rotation via the Pauli  $X$  matrix with dephasing in the  $Z$  basis. The long term behavior of this Lindbladian is depolarizing, as any state not in the  $Z$  basis becomes more mixed, and a state diagonal in the  $Z$  basis rotates to another basis. We apply  $\mathcal{L}$  to the input state  $|0\rangle\langle 0|$ . Again using continuity of relative entropy to a subalgebra restriction,

$$D(\Phi^t(|0\rangle\langle 0|)\|\hat{1}/2) \geq (1 - O(t^2 \log t))D(|0\rangle\langle 0|\|\hat{1}/2) . \tag{7}$$

This counterexample to RMLSI also hints at another feature: the quantum Zeno effect.

The nearest-neighbor chains of Counterexample 3.1 make it fairly intuitive why RMLSI must fail: the fixed point accounts for propagation of noise throughout the entire system, but the noise process itself takes time to propagate. As in the discrete case, short term dynamics may not sample enough of the long-term mixing process to induce decay at the expected rate. Counterexample 3.2 shows that as well as propagating through physical space, noise also takes time to propagate between bases. Though we do not see RMLSI, we might still expect strong decay estimates after some threshold time. Indeed, we will see by Section 3.2 that such estimates exist. First, we must address the Zeno effect.

Counterexample 3.2 is actually the continuous version of the original Zeno effect [MS77]. A continuous, measurement-like process blocks a quantum state's rotation out of its original basis. Less obvious is that Counterexample 3.1 also admits a Zeno-like effect: were one to tune up the noise strength toward infinity, the noised end would decouple from other qubits.

To better illuminate the connection between the Zeno effect and decay rates, we show a Zeno-like Theorem:

**Theorem 3.3.** *Let  $\mathcal{L}$  be a bounded Lindbladian and  $t > 0$  on a space with finite trace. For any quantum channel  $\Phi$  with  $\lambda$ -decay to non-rotating fixed point projector  $\mathcal{E}$  and  $k \in \mathbb{N}$ ,*

$$\|(\Phi \circ e^{-\mathcal{L}t/k})^k - e^{-\mathcal{E}\mathcal{L}\mathcal{E}t}\mathcal{E}\|_{\diamond} = \begin{cases} O(1/k) & \text{for } k \text{ large,} \\ O(1/\lambda k) & \text{for } k \text{ large, } \lambda \text{ small.} \end{cases}$$

*For any Lindbladian  $\mathcal{S}$  with  $\lambda$ -CMLSI to  $\mathcal{E}_0$ ,*

$$\|e^{-(\mathcal{S}+\mathcal{L})t} - e^{-\mathcal{E}\mathcal{L}\mathcal{E}t}\mathcal{E}\|_{\diamond} = O\left(\frac{1}{\lambda}\right).$$

Theorem 3.3 is a shortened version of Theorem B.19 shown in the Supplementary Information, which has explicit constants. For the discrete interruption setting, concrete bounds also appear as Proposition B.5 and Theorem B.17, each of which has explicitly calculated constants with a different tradeoff between generality and tightness. Though Theorem 3.3 is similar to results of [BFN<sup>+</sup>19, BFN<sup>+</sup>20, MR21], it differs in an essential way: rather than bounding Zeno convergence in terms of spectral properties of  $\Phi$  or an explicit constant multiplying  $\mathcal{S}$ , Theorem 3.3 bounds convergence in terms of CMLSI and decay constants. As seen in Example C.12 in the Supplementary Information, there are cases in which stronger decay does not arise from multiplicative comparability.

The continuous part of Theorem 3.3 highlights the self-restricting aspect of noise. Unless  $H$  commutes with  $\mathcal{E}_0$ , the Zeno limit will not coincide with the long-time fixed point. Hence strong CMLSI of the stochastic process actually suppresses decay to the overall fixed point. Here we let  $C_{cb}(\mathcal{E}_0)$  denote the Pimsner-Popa index of  $\mathcal{E}_0$  as recalled in Subsection 5.2. A primary motivation for revisiting generalized Zeno-like effects in this paper is the following:

**Theorem 3.4.** *Let  $\mathcal{L} = i[H, \cdot] + \mathcal{S}$  generate  $\Phi^t$ , where  $H$  is a Hamiltonian and  $\mathcal{S}$  a Lindbladian with  $\lambda_0$ -CMLSI to fixed point projector  $\mathcal{E}_0 \neq \mathcal{E}$ . Let  $\mathcal{E}$  denote the overall fixed point projector and  $R_t$  any persistent rotation. If there exists a  $t_0 > 0$  for which  $D(\Phi^t(\rho) \| R_t \mathcal{E}(\rho)) \leq e^{-\lambda t} D(\rho \| \mathcal{E}(\rho))$  for all  $t > t_0$ , then for sufficiently large  $\lambda_0$ ,  $\lambda = O(1/\sqrt{\lambda_0})$ .*

A technical version with explicit constants appears as Theorem C.7. Theorem 3.4 shows the emergence of an inverse relationship between  $\lambda$  and  $\lambda_0$  emerging from Zeno-like effects detailed in 3.3. We also show a general CMLSI converse:

**Theorem 3.5.** *Let  $(\Phi^t : t \in \mathbb{R}^+)$  be a continuous quantum Markov semigroup in the form of Equation (2) with stochastic generator  $\mathcal{S}$  having fixed point conditional expectation  $\mathcal{E}_0$ . Then*

$$D(\Phi^t(\rho) \| \mathcal{E}_0 \Phi^t(\rho)) \geq \exp(-C_{cb}(\mathcal{E}_0) \|\mathcal{S}\|_{\diamond} t/2) D(\rho \| \mathcal{E}_t(\rho)),$$

*where  $\mathcal{E}_t = R_{\exp(-iHt)} \mathcal{E}_0 R_{\exp(iHt)}$ .*

For detailed balance semigroups with no drift, Theorem 3.5 shows that decay does not completely eliminate relative entropy - there is always some remnant of the original state and its relative entropy to the fixed point subalgebra. Theorem 3.5 is however the key to showing that despite the restrictive influence of the Zeno effect, continuous quantum Markov semigroups with drift show exponential decay after finite time. Since fast convergence toward the Zeno limit



hinders decay toward the long-time fixed point, a speed limit on decay due to  $\mathcal{S}$  allows drift to spread noise across subspaces at a rate bounded above zero.

**3.2. Lower Bounds on Decay Rates.** In this Subsection, we show that despite the short-time effects illustrated by Counterexamples 3.1 and 3.2 as well as competition with Zeno-like effects, many processes still show exponential decay in the medium or long term. In particular, a process that applies unitary rotations along with decay-inducing subprocesses will after some time have decay properties determined by how its constituents combine.

**3.2.1. Decay + Drift Lindbladians.** The Zeno limit as the decay strength in Equation (2) becomes overwhelming and the long-time limit as  $t \rightarrow \infty$  converge to different points, so they cannot converge simultaneously.

Despite counterexamples to universal MLSI and the Zeno effect, we still expect exponential decay with estimable rate to emerge after finite time. When  $\mathcal{S}$  induces slow decay, the overall decay should obviously be correspondingly slow. As one continuously increases the strength of  $\mathcal{S}$  such as by taking  $\mathcal{S} \rightarrow \gamma\mathcal{S}$  for  $\gamma \geq 0$ , the overall decay rate for fixed  $t$  should at first ascend before again declining due to the Zeno effect. These extremes are distinct, as  $\gamma = 0$  corresponds to fully coherent time-evolution, while  $\gamma \rightarrow \infty$  converges to  $\mathcal{E}_0$ .

Let  $\beta_{2,\epsilon} = 1 - O(\epsilon)$  be defined as in Subsection 5.1 . We show a lower bound on the decay rate for decay+drift Lindbladians:

**Theorem 3.6.** *Let  $\mathcal{L}$  be a Lindbladian in the form of Equation (2) with stochastic generator  $\mathcal{S}$  and Hamiltonian  $H$ . Let  $\mathcal{E}_t := R_{\exp(-iHt)}\mathcal{E}_0R_{\exp(iHt)}$ . Let  $\mathcal{E}$  denote the invariant subspace under decay at all values of  $t$ . Assume that  $\mathcal{S}$  has  $\lambda$ -CMLSI and for given  $\tau \in \mathbb{R}^+$  that*

$$(1 - \epsilon)\mathcal{E} \leq_{cp} \left( \int_0^\tau e^{-C_{cb}(\mathcal{E}_0)\|\mathcal{S}\|_\diamond t/2} \mathcal{E}_t dt \right)^m \leq_{cp} (1 + \epsilon)\mathcal{E} , \quad (8)$$

*which is necessarily satisfied for  $\tau > 0$  with some  $m \in \mathbb{N}$ ,  $\epsilon \in (0, 1)$ , and  $c > 1$  in finite dimension. Then  $\exp(-\mathcal{L}\tau)$  has  $\beta_{2,\epsilon}\lambda/m$ -decay.*

To understand the assumption in Equation (8) and how this Theorem arises, we examine how distinct regimes compare qualitatively to the observations in Subsection 2.2.1. As in [BFN<sup>+</sup>19], we consider a Lindbladian of the form  $\mathcal{L} = i[H, \cdot] + \gamma\mathcal{S}$ , which attaches a multiplicative scalar factor  $\gamma > 0$  to  $\mathcal{S}$  in the decay + drift form. This  $\gamma$  factor allows us to tune the strength of the stochastic part, exploring different regimes. To simplify the analysis, we may take the factor of  $e^{-C_{cb}(\mathcal{E}_0)\|\mathcal{S}\|_\diamond t/2}$  outside of the integral, yielding that when

$$(1 - \epsilon)\mathcal{E} \leq_{cp} \left( \int_0^\tau \mathcal{E}_t dt \right)^m \leq_{cp} (1 + \epsilon)\mathcal{E} , \quad (9)$$

the channel  $\exp(-\mathcal{L}\tau)$  has  $\tilde{\lambda}$ -decay with

$$\tilde{\lambda} = e^{-m\gamma C_{cb}(\mathcal{E}_0)\|\mathcal{S}\|_\diamond \tau/2} \gamma \beta_{2,\epsilon} \lambda / m . \quad (10)$$

Equation (9) has the form of a continuous quasi-factorization inequality as in C.9. Indeed, the overall approach to proving Theorem 3.6 is to relate the problem to a kind of decay merging:

given a set of Lindbladians  $\mathcal{S}_t$  parameterized by time  $t$  and each having  $\lambda$ -CMLSI, the composite Lindbladian

$$\mathcal{S}_{tot} = \int_0^\tau \mathcal{S}_t dt \quad (11)$$

would have CMLSI with a constant depending on  $\lambda$  and  $\tau$  (see Equation (17) and Lemma C.9). Technically, one could optimize Theorem 3.6 further by redistributing measure in a more general way as in Lemma C.9, but here we aim to avoid this additional layer of complexity.  $\mathcal{L}$  however does not have the exact form of  $\mathcal{S}_{tot}$ : rather than apply effectively rotated versions of  $\mathcal{S}$  simultaneously,  $\mathcal{L}$  applies them sequentially. Theorem 3.5 shows that at time  $t$ , there is still some remnant of the original state at least for relative entropy. Hence we may apply decay merging as though different  $\mathcal{S}_t$  occurred simultaneously.

When  $\gamma$  is small compared to other relevant constants,  $e^{-m\gamma C_{cb}(\mathcal{E}_0)\|\mathcal{S}\|_\diamond\tau/2} \approx 1$ . In this regime,  $H$  fully rotates  $\mathcal{S}$  before much noise occurs. Equation 11 becomes a reasonable approximation to the noise imposed by  $\mathcal{L}$  over time  $\tau$ . Since  $\gamma$  is still small, the amount of overall noise is itself small. We may expand Equation (10) as  $\tilde{\lambda} = \gamma\beta_{2,\epsilon}\lambda/m - O(\gamma^2)$ , observing here that  $\tilde{\lambda}$  increases proportionally to  $\gamma$ . In Figure 2, this regime corresponds roughly to 0-1% depolarizing noise.

When  $\gamma$  is large, the exponential decay in  $\gamma$  dominates over the linear  $\gamma$  factor in Equation (10). This regime corresponds to 10-100% depolarizing noise in Figure 2. The large  $\gamma$  regime is well-described by Zeno-like bounds as in Theorem 3.3. Intuitively, stochastic components at small values of  $t$  leave little of the initial state intact, so  $\mathcal{L}$  differs strongly from the regime of Equation (11). In this regime, larger  $\gamma$  actually protects some information from its own spread, unless  $\mathcal{S}$  commutes with  $H$ .

The regime of strongest overall decay appears for intermediate values of  $\gamma$ , such as with 1-10% depolarizing noise in Figure 2. One may optimize Equation (10) for  $\gamma$  in this regime, though a better strategy involves optimizing  $\tau$ . Indeed, to calculate a decay constant for  $\exp(-\mathcal{L}t)$  with a given value of  $t$ , the value of  $(1 - \tilde{\lambda})^{\lfloor t/\tau \rfloor}$  might be smallest with  $\tau$  substantially less than  $t$ . Here we see eventual exponential decay. Strong decay relies on there existing values of  $\tau$  that sufficiently sample possible rotations while the system is reasonably close to its original state.

Though Theorem 3.6 agrees qualitatively with simulation, we expect the quantitative correspondence to be loose. The simulations of Subsection 2.2.1 use input states that are optimized to show the largest possible effects. In contrast, Theorem 3.6 trades away this optimality to derive bounds independent of the input state and with extremely coarse dependence on  $\mathcal{S}$  and  $H$ .

**3.2.2. Discrete Channel Compositions.** Analogously to decay merging for Lindbladians, we aim to show that a composition of channels  $\Phi_m \dots \Phi_1$  has decay properties that we can estimate through the individual channels' decay rates. If  $\Phi_1, \dots, \Phi_m$  contain unitary-like rotations and do not ultimately decay the state to one that is invariant under these rotations, then  $\Phi_m \dots \Phi_1$  may not converge to a unique fixed point. For example, if  $\Phi_j$  is a unitary from a finite set for all  $j$ , then the fixed point projection might average over all these unitaries and their inverses, but applying the unitaries in deterministic order would never converge to this average.

The following result is a decay merging Theorem for composed channels:

**Theorem 3.7.** *Let  $\Phi_1, \dots, \Phi_m$  be quantum channels with respective fixed point conditional expectations  $(\mathcal{E}_j)_{j=1}^m$  and fixed point rotations  $R_m, \dots, R_1$ . Assume that each  $\Phi_j$  has (complete)  $\lambda_j$ -decay. If*

$$(1 - \epsilon)R_m \dots R_1 \mathcal{E} \leq_{cp} R_m \mathcal{E}_m \dots R_1 \mathcal{E}_1 \leq_{cp} (1 + \epsilon)R_m \dots R_1 \mathcal{E} \quad (12)$$

for constants  $c > 1$  and  $\zeta \in (0, 1)$ , then  $\Phi_m \circ \dots \circ \Phi_1$  has (complete)  $(\min_j \lambda_j)\beta_{2,\epsilon}$ -decay.

For a probabilistic distribution  $(p_j)_{j=1}^m$ , let  $\Phi := \sum_j p_j \Phi_j$ . If

$$(1 - \epsilon)\mathcal{E} \leq_{cp} \left( \sum_j p_j \mathcal{E}_j \right)^k \leq_{cp} (1 + \epsilon)\mathcal{E}, \quad (13)$$

then  $\Phi$  has (complete)  $\beta_{2,\epsilon} \min_j p_j \lambda_j / 2k$ -decay. In finite dimension when  $R_j$  is the identity matrix for each  $j \in 1 \dots m$ , the condition of Equation (13) is necessarily satisfied for some  $k$  and any probability distribution  $(p_j)$ .

Theorem 3.7 allows us to derive decay estimates for single steps in a process from the properties of long sequences of corresponding conditional expectations. In Example 5.3, examine how channels in the form of the second part of Theorem 3.7 converge to  $T$ -designs. While Haar random unitaries are often useful in studying topics ranging from computational complexity to high-energy physics, they are prohibitively complex to generate [Aar16]. In contrast, local, polynomial size circuits often suffice to construct approximate  $T$ -designs [BHH16, HM18], which approximately reproduce the first  $T$  statistical moments of Haar random unitaries. These results show the approximate  $T$ -design property in the sense of semidefinite matrix ordering or norm distance from an exact  $T$ -design. While these properties often suffice to show relative entropy decay for the overall circuits, the results for how individual gates or layers are not as strong. Via Theorem 3.7, we construct a constant-depth channel converging to a  $T$ -design after  $O(n)$  repetitions such that a single use has per-step relative entropy decay.

Theorem 3.7 is a simplification of Theorem C.4. The idea of Theorem 3.7 is again based on decay merging: if we have decay estimates for the individual channels and can compare their (possibly rotating) fixed point projectors to an overall non-decaying subspace, then we have decay estimates for their composition. A key aspect of Theorem 3.7 is that the cp-order assumptions are on compositions of the fixed point projectors, not the original channels themselves. In the first part of the Theorem, there is no general guarantee that the condition is satisfied. For example, we did not assume that every value of  $j$  even appears in the sequence. Unlike Theorem 3.6, discrete sequences of channels do not have the extra continuity structure that would ensure every subspace projector is eventually encountered. In contrast, the second part of Theorem 3.7 applies channels in a parallel-like way via convex combination, avoiding the time-dependent penalties of Theorem 3.6. In the absence of persistent rotations, a setting analogous to that of GNS detailed balance for Lindbladians, the weighted averaging also recovers the assurance of eventual decay. The discrete setting does not necessarily encounter Zeno-like effects in the same way as the continuous setting, but we again find that time-dependent, sequential effects may protect subspaces from noise.

#### 4. DISCUSSION AND CONCLUSIONS

While findings herein complicate decay estimation, they are correspondingly optimistic for noise reduction in quantum technology. When local noise becomes overwhelmingly strong, it often begins to block interactions, restricting itself to its original location or basis.

If one continuously monitors or strongly dephases an otherwise closed system, the generalized Zeno effect will suppress internal dynamics that would otherwise shift away from that basis. Hence instead of spreading into a stochastic mixture of possible paths, the system's state will follow a deterministic trajectory according to possibly reduced dynamics that appear diagonal in the selected basis.

One may wonder why CMLSI and decay bounds seem to work best in relative entropy, whereas Zeno-like bounds are in diamond norm. One may translate between these settings at a logarithmic cost in dimension or subspace indices using continuity bounds such as Pinsker's inequality and the Alicki-Fannes inequality. Nonetheless, there are probably reasons why decay takes certain forms. As relative entropy is extensive on tensor product compositions of states, its value may grow with system size. The higher starting value of relative entropy and its relation to composition leaves more room for CMLSI-like estimates. In contrast, the trace or diamond norm has a maximum of 1 (or 2, depending on normalization), which in many-body systems is technically achievable by a small subsystem. Hence in the absence of strong, global decay, a large system might reasonably preserve its one-norm distance from a fixed point until very late. CMLSI is particularly useful in yielding non-trivial decay in arbitrarily small time, enabling compositions of infinitesimal intervals.

Future studies may seek to extend beyond the decay+drift form. There is a general way to decompose a finite-dimensional Lindbladian into uniquely defined Hamiltonian and dissipative subprocess [HS21]. It is not clear whether the dissipative component will satisfy the detailed balance condition used herein or even a general notion of rotation freeness. Nonetheless, such a decomposition is suggestive. One may ask whether the canonically defined dissipative part of a Lindbladian always has CMLSI or other forms of exponential decay. A broader open problem is to improve decay estimates when the fixed point subspace is lower rank than the input subspace, such as under damping noise. While relative entropy decay is strong and useful for unital noise, relative entropy to a low-rank state might be infinite even when the input is by other measures close to the fixed point.

#### 5. METHODS

**5.1. Experimental and Numerical Methods.** Simulations in Subsection 2.1 were run in Qiskit dynamics using the Lindbladian solver. Von Neumann entropies were calculated using Qiskit's 'quantum\_info.entropy' subroutine and subtracted from 4.0 to obtain the relative entropy with respect to the completely mixed fixed point state. We denote the (unnormalized) Pauli matrices

$$X = \begin{pmatrix} 0 & 1 \\ 1 & 0 \end{pmatrix}, Y = \begin{pmatrix} 0 & -i \\ i & 0 \end{pmatrix}, Z = \begin{pmatrix} 1 & 0 \\ 0 & -1 \end{pmatrix}.$$

The simulations in Subsubsection 2.2.1 were conducted using Qiskit. To approximate continuous dynamics on a discrete, circuit-based backend, we simulate the Trotter expanded version

$$(\exp(-itH/k) \exp(-t\gamma\mathcal{S}/k))^k .$$

The unitary rotation was implemented as a parameterized RZX gate, and the depolarizing noise using a Qiskit *NoiseModel* in the *AerSimulator*. These simulations were carried out using the ‘density\_matrix’ method with 8192 shots and channels inferred using Qiskit’s ‘process\_tomography\_circuits’ and ‘process\_tomography\_fitter’ subroutine and class for the single ‘B’ qubit. The ‘cts’ simulation was run using Qiskit Dynamics with the Lindbladian solver using a Bell state input to directly compute the Choi matrix.

In simulation, one may program the channel  $\Phi_{(k)}$  almost exactly. In experiment, there are several challenges. First, IBMQ devices do not natively implement depolarizing channels, since depolarizing is what one typically aims to avoid in computation or communication. Second, unintended noise on qubit  $B$  may induce mixture independently from any process on  $A$ , diluting the Zeno effect’s protection. Third, small, two-qubit rotations also differ from the typical use case of gate-based quantum computers. For the experiment, we apply the following procedure:

- (1) The device is initialized in the computational basis  $|0\dots 0\rangle$  state.
- (2) Channel tomography preparation gates are applied to qubit  $B$ .
- (3) The following sequence of steps is repeated for  $k$  rounds:
  - (a) Apply  $\mathcal{E}_0$ :  $S_Z$  gates are applied to each of two auxiliary qubits. One  $CX$  gate is applied from the first auxiliary to  $A$ . One Hadamard is applied to  $A$ . One  $CX$  is applied from the second auxiliary to  $A$ . Reset operations begin on both auxiliaries.
  - (b) Apply  $\Phi_{ZX(\pi/(2k))}$ : using the Qiskit class `RZXCalibrationBuilder` and `OpenPulse` access, a pulsed implementation of  $\Phi_{ZX(\pi/(2k))}$  is applied from qubit  $A$  to qubit  $B$ .
  - (c) Wait for the next cycle: between each application of  $\Phi_{ZX(\pi/(2k))}$  or the beginning or end of the circuit, dynamical decoupling is applied to  $B$  via a pair of  $X$  gates inserted via Qiskit’s dynamical decoupling routine.
- (4)  $\mathcal{E}$  is applied again without the reset operations.
- (5) Channel tomography gates are applied to qubit  $B$ , and it is measured. Qubit  $A$  is assumed to be fully depolarized, as the state of it and the auxiliaries is discarded.

For small values of  $k$ , there is an initial increase in fidelity of  $\Phi_{(k)}$  with the identity channel on  $B$ . Nonetheless, fidelity quickly begins to drop. Experimental results then begin to diverge from noiseless simulation. Though the pulse-based  $\Phi_{ZX(\pi/(2k))}$  yields improved performance compared with the default mapping to native gates, it does not decline as  $1/k$  but enters a regime of diminishing returns (see [SBEP21] for details). Furthermore, each application of  $\mathcal{E}_0$  requires approximately  $1\mu s$  waiting for the auxiliary qubits to reset. Based on the reported  $T_1$  and  $T_2$  for qubit  $B$ , one may reasonably estimate that each application of  $\mathcal{E} \circ \Phi_{ZX(\pi/(2k))}$  induces on the order of  $1 - 2\%$  infidelity via passive noise. The effects of unintended hardware noise increase with  $k$ , contrasting the protective scaling of the Zeno effect. For  $k > 5$ , unintended noise appears to dominate. Not only does fidelity of  $\Phi_{(k)}$  with the identity channel quickly begin

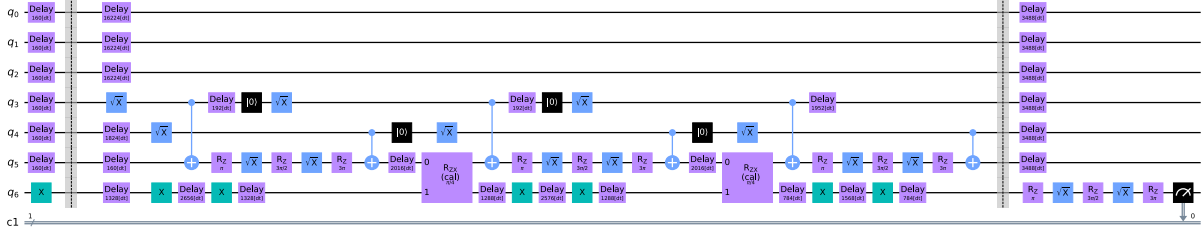


FIGURE 4. The circuit to apply the channel  $\Phi_{(2)}$ . Qubit  $q_6$  on the *ibm\_lagos* serves as  $B$ ,  $q_5$  as  $A$ , and  $q_3$  and  $q_4$  as auxiliaries. Figure created using IBM Quantum, generated using Qiskit and the Matplotlib backend. Gates within the two barriers apply  $\Phi_{(k)}$ , while gates surrounding the barriers are inserted by Qiskit’s channel tomography.

to decrease, but fidelity with the long-time fixed point (in which  $B$  is fully dephased in the  $X$  basis) also drops quickly. See Figure 5 in Appendix D for raw results.

To bypass unintended noise, we apply a principle inspired by error mitigation. With some knowledge of the form of noise, it is possible to extrapolate to a lower-noise case. Typical error mitigation schemes may attempt to characterize the effect of readout and gate noise on observed measurement outcome statistics, then apply various forms of approximate matrix inverse to estimate the pre-noised statistics. In our scenario, an analogous procedure is greatly simplified by the fact that most forms of device noise do not resemble dephasing in the  $X$  basis. Given a  $4 \times 4$  Choi matrix  $M$  from process tomography on a single qubit, one may model the effect of incoherently applying the  $X$  operator by

$$\frac{|M_{14}| + |M_{23}|}{|M_{14}| - |M_{23}|} = \exp(\chi t), \quad (14)$$

where  $\chi \in \mathbb{R}^+$  is a parameter controlling the strength of  $X$ -basis dephasing noise. One may see via the “ $D^4$ ” model introduced in [LSI<sup>+</sup>22] that a combination of  $Z$ -basis dephasing, amplitude damping, depolarizing, and coherent phase drift do not directly affect the ratio given in Equation (14). Hence we may extract the expected effect of  $\Phi_{(k)}$  independently from common forms of noise in superconducting qubits. To extract the Zeno effect from the noise induced by real hardware, we solve for  $\chi$  as in Equation (14) via the Choi matrix from process tomography, then use  $\chi$  to construct a purely dephasing channel.

At  $k = 16$ ,  $|M_{14}| - |M_{23}| < 0$ , resulting in a negative argument to the logarithms used to solve Equation (14) for  $\chi$ . That this difference is negative suggests stronger  $X$  rotation than mere dephasing. By itself, this over-rotation in  $X$  may result from passive drift, from overrotation in the application of  $\Phi_{ZX(\pi/(2k))}$ , or even from small fluctuations in device parameters fluctuations when both  $|M_{14}|$  and  $|M_{23}|$  are small due to unintended  $Z$ -basis dephasing, amplitude damping, and depolarizing noise. Based on the unexpectedly fast convergence observed in Figure 3.(1) and Figure 3.(3), it appears that a buildup in calibration errors is likely. This explanation is consistent with the difficulty in calibrating  $\Phi_{ZX(\pi/(2k))}$  for large values of  $k$ . Since experiments

with  $k > 15$  may fail to reflect intended parameters, we truncate the results presented in Figure 3 to earlier points.

**5.2. Theoretical Methods.** By  $\mathbb{B}(\mathcal{H})$  we denote the space of bounded operators on Hilbert space  $\mathcal{H}$ , and by  $\mathcal{D}(\mathcal{H})$  we denote the space of densities. By  $\hat{1}$  we denote the identity matrix. For a unitary matrix  $U$ , we denote by  $R_U$  the channel that applies that unitary matrix via conjugation such that  $R_U(X) := UXU^\dagger$  for any  $X \in \mathbb{B}(\mathcal{H})$ . If there is a family of unitaries  $(U_j)$ , we may denote  $R_j := R_{U_j}$  when it is clear from context. A quantum channel is a completely positive, trace-preserving map, usually denoted by  $\Phi, \Psi$ , or  $\Theta$ . For products of quantum channels, we use left multiplication to denote composition or the “ $\circ$ ” symbol to optimize readability, e.g.  $\Phi\Psi(\rho) = \Phi(\Psi(\rho)) = \Phi \circ \Psi(\rho)$ . We often use the diamond norm to compare quantum channels, denoted  $\|\cdot\|_\diamond$ . See Appendix A for more information on norms used in this paper.

Relative entropy inequalities herein are restricted to finite dimension, though they should in principle extend to infinite dimension with re-derivation of some referenced inequalities. The Zeno-like norm bounds derived in Appendix B in principle generalize to some infinite-dimensional settings, but that is not the focus of this paper.

A *quantum Markov semigroup* (QMS) is a family of channels  $(\Phi^t)$  for  $t \in \mathbb{R}^+$  (continuous case) or  $t \in \mathbb{N}$  (discrete case) with the essential property that  $\Phi^t\Phi^s = \Phi^{t+s}$ . For any quantum channel  $\Phi$ ,  $(\Phi^t : t \in \mathbb{N})$  is a discrete semigroup of powers of the channel. Any continuous QMS has an adjoint Lindbladian generator  $\mathcal{L}$  such that  $\Phi^t = \exp(-t\mathcal{L})$  for any  $t \in \mathbb{R}^+$ . For a Hamiltonian  $H$ , we denote by  $i[H, \cdot]$  the operator given by  $i[H, \cdot](x) := i[H, x]$  for an operator  $x$ . Hence  $R_{\exp(-iHt)} = \exp(-i[H, \cdot])$ . A Lindbladian generalizes Hamiltonian time-evolution to open systems.

For a normal, faithful density  $\omega \in \mathcal{D}(\mathcal{H})$ , the GNS inner-product with respect to  $\omega$  is defined for  $x, y \in \mathbb{B}(\mathcal{H})$  as  $\langle x, y \rangle_\omega = \text{tr}(\omega x^*y)$  in a tracial setting. We say that a Lindbladian has *GNS detailed balance* or that  $\mathcal{L}$  is *GNS self-adjoint* when  $\mathcal{L}$  is self-adjoint with respect to the GNS inner product for an implied (or explicitly written) invariant density  $\omega$ . Formally, the standard Lindbladian is  $\mathcal{L}^*$ , the adjoint of  $\mathcal{L}$  with respect to the trace.

Any Lindbladian with GNS detailed balance has a fixed point subspace  $\mathcal{N}_\omega$  contained in its fixed point von Neumann algebra  $\mathcal{N}$  [CM17]. There is a fixed point projector  $\mathcal{E}$  to  $\mathcal{N}_\omega$ , the pre-adjoint of a conditional expectation  $\mathcal{E}^*$  with respect to the trace<sup>2</sup>. Some additional properties of  $\mathcal{E}$  are described in Appendix A. We also recall the Pimsner-Popa subalgebra indices, which we denote for subspace projections,

$$C(\mathcal{E}) = \inf\{c > 0 \mid \rho \leq c\mathcal{E}(\rho) \forall \rho \in \mathcal{M}_*\}, \quad C_{cb}(\mathcal{E}) = \sup_{n \in \mathbb{N}} C(\mathcal{E} \otimes \text{Id}^n).$$

as considered in [GJL20b, GR21] and originally by Pimsner and Popa [PP86] as a finite-dimensional analog of the Jones index [Jon83]. When  $\mathcal{E}$  has is GNS self-adjoint with respect to density  $\omega$ ,  $C_{cb}(\mathcal{E}) \leq d^2\omega_{\min}^{-1}$ , where  $d$  is the dimension of the space and  $\omega_{\min}^{-1}$  the minimum eigenvalue of  $\omega$ .

<sup>2</sup>As with the Lindbladian, we denote by  $\mathcal{E}$  the completely positive, trace-preserving or Schrödinger picture quantum channel, and by  $\mathcal{E}^*$  its adjoint, which differs in convention from the von Neumann algebra literature.

A starting point for this work is the quantum version of the modified logarithmic Sobolev inequality (MLSI) introduced by Kastoryano and Temme [KT13]. Stochastic versions of this inequality appear in earlier literature [AMTU98, BT03]. MLSI differs from but was inspired by the earlier notion of logarithmic Sobolev inequalities [Gro75b, Gro75a]. An important, more recent observation is that while the canonical log-Sobolev inequality fails for semigroups that lack a unique fixed point state [BR18], the modified version fares better [Bar17]. This observation motivates the notion of a complete modified logarithmic-Sobolev inequality (CMLSI) [GJL20a]. A finite-dimensional semigroup generated by  $\mathcal{L}$  has  $\lambda$ -CMLSI iff

$$D((e^{-\mathcal{L}t} \otimes \hat{1}^B)(\rho) \| (\mathcal{E} \otimes \hat{1}^B)(\rho)) \leq e^{-\lambda t} D(\rho \| (\mathcal{E} \otimes \hat{1})(\rho)) \quad (15)$$

for all extensions by a finite-dimensional auxiliary subsystem  $B$ . CMLSI with some constant is known for all finite-dimensional quantum Markov semigroups having GNS detailed balance with respect to a faithful state. This result was derived in a self-contained way in [GR21]. It was simultaneously derived in [GJL21] for semigroups that are self-adjoint with respect to the trace, which via [JLR19] also extends to all finite-dimensional semigroups with detailed balance.

An important tool is the multiplicative relative entropy comparison from earlier work. Let  $\rho$  be a density and  $\mathcal{E}, \Phi$  be quantum channels such that  $\Phi(\rho) \leq c\mathcal{E}(\rho)$  for constant  $c > 1$ , and let  $\zeta \in (0, 1)$ . Furthermore, let  $\Phi\mathcal{E} = \mathcal{E}$ . Then

$$D(\rho \| (1 - \zeta)\mathcal{E}(\rho) + \zeta\Phi(\rho)) \geq \beta_{c,\zeta} D(\rho \| \mathcal{E}(\rho)) \text{ for } \beta_{c,\zeta} = 1 - O(c\zeta). \quad (16)$$

A concrete value of  $\beta_{c,\zeta}$  is determined in [LaR21], from which we see that

$$\beta_{c,\zeta} \geq \frac{1}{1 + \zeta(c+1) + 2\zeta^2(c-1)} \left( 1 - 3\zeta(2 + \zeta) \frac{(c-1)^2}{c(\ln c - 1) + 1} - 8\zeta - 2\zeta^2 \right).$$

One may also use the some of the approximate tensorization estimates from [GR21]. A common form of Equation (16) with one parameter states that if a channel  $\Psi$  has that  $\Psi\mathcal{E} = \mathcal{E}\Psi = \mathcal{E}$  and  $(1 - \epsilon)\mathcal{E} \leq \Phi \leq (1 + \epsilon)\mathcal{E}$ , then  $D(\rho \| \Psi(\rho)) \geq \beta_{2,\epsilon} D(\rho \| \mathcal{E}(\rho))$ , and  $\beta_{2,\epsilon} = 1 - O(\epsilon)$ .

Because CMLSI yields tensor-stable decay rate bounds on processes such as decoherence [BJL<sup>+</sup>21] and thermal equilibration [BCG<sup>+</sup>21], concrete estimates of involved constants are valuable and have practical relevance. A method of particular relevance noted in [LaR21, BCR22] allows one to build up MLSI estimates for a complicated system from its constituents. In particular, let  $\mathcal{L}_1, \dots, \mathcal{L}_m$  be Lindbladian generators with detailed balance and respective fixed point projector  $\mathcal{E}_1, \dots, \mathcal{E}_m$ , and  $\mathcal{L} = \mathcal{L}_1 + \dots + \mathcal{L}_m$  with fixed point projector  $\mathcal{E}$ . If each  $\mathcal{L}_j : j \in 1 \dots m$  has (C)MLSI with respective constant at least  $\lambda_j$  and if

$$\sum_{j=1}^m \alpha_j \lambda_j D(\rho \| \mathcal{E}_j(\rho)) \geq D(\rho \| \mathcal{E}(\rho)), \quad (17)$$

then  $\mathcal{L}$  has  $1/(\sum_j \alpha_j)$ -(C)MLSI. We call this trick *decay merging*. The condition of Equation (17) is known as quasi-factorization or approximate tensorization. Quasi-factorization was first shown for the classical case in [Ces01], generally proven for the quantum relative entropy in [GR21], and refined in [LaR21, BCR22]. We use versions of (17) from [LaR21], which follow from (16) with iterated compositions of conditional expectations.



CMLSI may technically fail if the fixed point subspace contains persistent rotations. To account for drifting fixed points of discrete channels  $\Phi_1, \dots, \Phi_m$ , we modify the assumed decay to fixed point subalgebras such that for each  $j \in 1..m$ , there is a unitary  $U_j$  such that (denoting  $R_j := R_{U_j}$ )

$$\Phi_j \mathcal{E} = \mathcal{E} \Phi_j = R_j \mathcal{E} = \mathcal{E} R_j . \quad (18)$$

for some common  $\mathcal{E}$ . We may further assume that each  $\Phi_j$  has its own fixed point expectation  $\mathcal{E}_j$  and corresponding  $U_j$  such that

$$\Phi_j \mathcal{E}_j = \mathcal{E}_j \Phi_j = R_j \mathcal{E}_j = \mathcal{E}_j R_j , \quad (19)$$

and  $\Phi_j^r \rightarrow R_j^r \mathcal{E}_j$  as  $r \rightarrow \infty$ . Under these assumptions,  $U_j$  accounts for the invertible drift that is not eliminated by stochastic decay. We may deduce from Equation (18) that

$$\Phi_m \dots \Phi_1 \mathcal{E} = U_m \dots U_1 \mathcal{E}$$

and from Equation (19) that  $\mathcal{E}_j \mathcal{E} = \mathcal{E}$  for each  $j$ .

**Definition 5.1.** *A channel  $\Phi$  has rotated decay with constant lambda ( $\lambda$ -decay) if  $\Phi^r \rightarrow R_U \mathcal{E}$  for some unitary  $U$  and conditional expectation  $\mathcal{E}$  such that*

$$\Phi \mathcal{E} = \mathcal{E} \Phi = R_U \mathcal{E} = \mathcal{E} R_U ,$$

and

$$D(\Phi(\rho) \| R_U \mathcal{E}(\rho)) \leq (1 - \lambda) D(\rho \| \mathcal{E}(\rho)) .$$

We say  $\Phi$  has complete  $\lambda$ -decay when  $\lambda$ -decay holds for all extensions by an auxiliary system.

Analogously to Definition 5.1, we define a continuous analog of MLSI for Lindbladians with a rotating protected subspace.

**Definition 5.2 (RMLSI).** *A quantum Markov semigroup  $\Phi^t$  and associated Lindbladian generator obey rotated MLSI ( $\lambda$ -RMLSI) if for all  $t \in [0, \infty)$ ,*

$$D(\Phi^t(\rho) \| \mathcal{E}(R^t(\rho))) \leq e^{-\lambda t} D(\rho \| \mathcal{E}(\rho))$$

for some continuously parameterized unitary  $R^t$  such that  $\Phi^t \mathcal{E} = \mathcal{E} \Phi^t = R^t \mathcal{E} = \mathcal{E} R^t$ . It has  $\lambda$ -CRMLSI if  $\lambda$ -RMLSI holds under extension by an arbitrary auxiliary system.

The necessity of allowing rotation in Definition 5.2 is illustrated by Example C.11 in the Supplementary Information.

Theorem 3.3 is proven in Section B within the Supplementary information. The primary argument of the proof is shows that the first order terms in Taylor series for the original dynamics and Zeno limit are equivalent after expanding in both the number of discrete steps ( $k$  in Theorem 3.3) and a matrix order comparison parameter determined by the decay constant. The result then follows from analytically and combinatorially bounding the higher-order terms in both of these parameters. To derive the continuous case, we use a Kato-Suzuki-Trotter formula in the  $k \rightarrow \infty$  limit.

The relative entropy decay Theorems in Section 3.2 both follow from variations on the decay merging trick as described in [LaR21] and in [BCR22]. Theorem 3.7 applies the same principle

as in earlier decay merging proofs: using the chain rule of relative entropy, one may add up the relative entropy decay subtractions from each channel's  $\lambda$ -decay and then apply a quasi-factorization / approximate tensorization inequality of the form in Equation (17) to show that these contributions add up to a multiple of the final entropy.

Theorem 3.6 is actually more subtle because of the possibility for Zeno-like effects to block decay to the long-time fixed point subspace. A counter-intuitive consequence of Theorem 3.3 is that a chain of conditional expectations may approach the action of a unitary on a particular subspace. Let  $\mathcal{E}_t := R_{\exp(-iHt)} \circ \mathcal{E}_0 \circ R_{\exp(iHt)}$  for Hamiltonian  $H$  and any  $t \in \mathbb{R}$ . Note that for any  $k \in \mathbb{N}$ ,  $\mathcal{E}_t \mathcal{E}_{t-1/k} \dots \mathcal{E}_{1/k} = R_{\exp(-iHt)} \circ (\mathcal{E}_0 R_{\exp(iHt/k)})^k$ . As a direct consequence,

$$\lim_{k \rightarrow \infty} \mathcal{E}_t \mathcal{E}_{t-1/k} \dots \mathcal{E}_{1/k} \mathcal{E}_0 = R_{\exp(i(\mathcal{E}_0(H)-H)t)} \circ \mathcal{E}_0 \quad (20)$$

What's surprising about this effect is that  $\mathcal{E}_0$  and hence each  $\mathcal{E}_t, \dots, \mathcal{E}_{1/k}$  is a self-adjoint, mixing conditional expectation. By its self-adjointness, one may consider each such channel to be rotation-free. Yet in the continuum limit, a chain of such channels approaches a unitary rotation following  $\mathcal{E}_0$ . The generalized Zeno effect thereby makes clear why Equation (53) from Theorem 3.7 does not yield a Theorem like 3.6 in the continuum limit.

Instead, to prove Theorem 3.6, we use Theorem 3.5 with Equation (17) to show that combined entropy subtractions from  $\lambda$ -CMLSI at different times still compare with the original entropy of the input state to its fixed point. The cost of this approach is the exponential penalty in the time, norm of the stochastic part of the generator, and Pimsner-Popa index of  $\mathcal{E}_0$ . In specific scenarios, one might substitute a stronger decay converse bound than Theorem 3.5 to obtain a stronger decay bound than Theorem 3.6. It remains open whether there is a generally stronger bound. Theorem 3.3 implies that there must be some penalty in terms of the stochastic part's decay strength, because the process cannot be arbitrarily close to its Zeno limit while also decaying arbitrarily fast toward its long-time fixed point unless they are compatible (such as when  $H$  commutes with  $\mathcal{E}_0$ ).

Finally, we consider the  $T$ -design example in detail.

**Example 5.3** (Steps of Approximate T-Designs). Let

$$\Psi_{(n,d,T),\nu}(\rho) := \int_U U^{\otimes T} \rho (U^*)^{\otimes T} d\nu \quad (21)$$

for any input density  $\rho$  on a system of dimension  $d^{nT}$  such that  $d$  is a local qudit dimension,  $n$  is the number of such qudits, and  $T$  is the number of copies of the  $n$ -qudit system. A strong,  $\epsilon$ -approximate unitary  $T$ -design on  $n$  qudits is a measure  $\nu$  on  $U(d^n)$  such that

$$(1 - \epsilon) \Psi_{(n,d,T),Haar} \leq_{cp} \Psi_{(n,d,T),\nu} \leq_{cp} (1 + \epsilon) \Psi_{(n,d,T),Haar} . \quad (22)$$

The main result of [BHH16, HM18] is how random circuits constructed out of 2-qudit unitaries form approximate  $T$ -designs. As [BHH16, Corollary 6], it was shown that 2-qudit random unitaries applied in parallel on a one-dimensional, nearest-neighbor lattice form  $\epsilon$ -approximate  $T$ -designs in depth  $O(n)$ . In particular, let

$$\Theta_\mu^A := \Psi_{(2,d,T),\mu}^{(1,2)} \otimes \dots \otimes \Psi_{(2,d,T),\mu}^{(n-1,n)}, \text{ and } \Theta_\mu^B := \Psi_{(2,d,T),\mu}^{(2,3)} \otimes \dots \otimes \Psi_{(2,d,T),\mu}^{(n-2,n-1)},$$

where the upper indices denote the qudits on which each channel is applied. This architecture applies  $(\Theta_\mu^A \circ \Theta_\mu^B)^{O(n)}$  and achieves a  $T$ -design with calculated constants when  $\mu$ . As shown in [BHH16, Corollary 7], non-Haar measures can also form  $T$ -designs in  $O(n)$  depth with an implicit constant.

Theorem 3.7 implies that the channel  $\Theta_\mu^{A+B} := (\Theta_\mu^A + \Theta_\mu^B)/2$  has  $\lambda$ -decay with  $\lambda = \Omega(1/n)$ . A power of  $\Theta_\mu^{A+B}$  is a convex combination of channels with a binomially distributed number of switching points between  $\Theta^A$  and  $\Theta^B$ , so most terms in the combination apply linearly many powers of  $\Theta_\mu$ . Hence this composition compares with the parallel architecture as in [BHH16, Corollary 6]. As  $\Theta_\mu^{A+B}$  expands as a sum of sequences of channels from  $\{\Theta_\mu^A, \Theta_\mu^B\}$ , it satisfies the conditions of the second part of Theorem 3.7. Using the properties of the eventual  $T$ -design constructed via  $O(n)$  steps, we obtain  $O(1/n)$ -decay for the single step  $\Theta_\mu^{A+B}$ . This decay of relative entropy does not follow immediately from the tensor-product expander bounds given in [BHH16] or the norm bounds in [HM18].

A continuous analog to this example appears in [GR21].

## 6. ACKNOWLEDGEMENTS

We thank John Smolin and Marius Junge for helpful feedback. We acknowledge the use of IBM devices through the researcher access program and the IBM Postdoc program at the Chicago Quantum Exchange.

## REFERENCES

- [Aar16] Scott Aaronson, *The Complexity of Quantum States and Transformations: From Quantum Money to Black Holes*, Tech. Report 109, 2016.
- [AMTU98] Anton Arnold, Peter Markowich, Giuseppe Toscani, and Andreas Unterreiter, *On logarithmic Sobolev inequalities, Csiszar-Kullback inequalities, and the rate of convergence to equilibrium for Fokker-Planck type equations*, 77 (en).
- [Bar17] Ivan Bardet, *Estimating the decoherence time using non-commutative Functional Inequalities*, arXiv:1710.01039 [math-ph, physics:quant-ph] (2017), arXiv: 1710.01039.
- [BCG<sup>+</sup>21] Ivan Bardet, Ángela Capel, Li Gao, Angelo Lucia, David Pérez-García, and Cambyse Rouzé, *Entropy decay for Davies semigroups of a one dimensional quantum lattice*, arXiv:2112.00601 [cond-mat, physics:math-ph, physics:quant-ph] (2021), arXiv: 2112.00601.
- [BCR22] Ivan Bardet, Ángela Capel, and Cambyse Rouzé, *Approximate Tensorization of the Relative Entropy for Noncommuting Conditional Expectations*, Annales Henri Poincaré **23** (2022), no. 1, 101–140 (en).
- [BDS21] Simon Becker, Nilanjana Datta, and Robert Salzmänn, *Quantum Zeno Effect in Open Quantum Systems*, Annales Henri Poincaré (2021) (en).
- [BFN<sup>+</sup>19] Daniel Burgarth, Paolo Facchi, Hiromichi Nakazato, Saverio Pascazio, and Kazuya Yuasa, *Generalized Adiabatic Theorem and Strong-Coupling Limits*, Quantum **3** (2019), 152 (en-GB), Publisher: Verein zur Förderung des Open Access Publizierens in den Quantenwissenschaften.
- [BFN<sup>+</sup>20] ———, *Quantum Zeno Dynamics from General Quantum Operations*, Quantum **4** (2020), 289 (en-GB), Publisher: Verein zur Förderung des Open Access Publizierens in den Quantenwissenschaften.
- [BHH16] Fernando G. S. L. Brandão, Aram W. Harrow, and Michał Horodecki, *Local Random Quantum Circuits are Approximate Polynomial-Designs*, Communications in Mathematical Physics **346** (2016), no. 2, 397–434 (en).

- [BJL<sup>+</sup>21] I. Bardet, M. Junge, N. LaRacuate, C. Rouzé, and Daniel Stilck França, *Group transference techniques for the estimation of the decoherence times and capacities of quantum Markov semigroups.*, IEEE Transactions on Information Theory (2021), 1–1, Conference Name: IEEE Transactions on Information Theory.
- [BR18] Ivan Bardet and Cambyse Rouzé, *Hypercontractivity and logarithmic Sobolev Inequality for non-primitive quantum Markov semigroups and estimation of decoherence rates*, arXiv:1803.05379 [math-ph, physics:quant-ph] (2018), arXiv: 1803.05379.
- [BT03] Sergey Bobkov and Prasad Tetali, *Modified log-sobolev inequalities, mixing and hypercontractivity*, Proceedings of the thirty-fifth annual ACM symposium on Theory of computing (New York, NY, USA), STOC '03, Association for Computing Machinery, June 2003, pp. 287–296.
- [BZ18] Norbert Barankai and Zoltán Zimborás, *Generalized quantum Zeno dynamics and ergodic means*, arXiv:1811.02509 [math-ph, physics:quant-ph] (2018), arXiv: 1811.02509.
- [Ces01] Filippo Cesi, *Quasi-factorization of the entropy and logarithmic Sobolev inequalities for Gibbs random fields*, Probability Theory and Related Fields **120** (2001), no. 4, 569–584 (en).
- [CM17] Eric A. Carlen and Jan Maas, *Gradient flow and entropy inequalities for quantum Markov semigroups with detailed balance*, Journal of Functional Analysis **273** (2017), no. 5, 1810–1869.
- [FLP04] P. Facchi, D. A. Lidar, and S. Pascazio, *Unification of dynamical decoupling and the quantum Zeno effect*, Physical Review A **69** (2004), no. 3, 032314, Publisher: American Physical Society.
- [GJL20a] Li Gao, Marius Junge, and Nicholas LaRacuate, *Fisher Information and Logarithmic Sobolev Inequality for Matrix-Valued Functions*, Annales Henri Poincaré **21** (2020), no. 11, 3409–3478 (en).
- [GJL20b] ———, *Relative entropy for von Neumann subalgebras*, International Journal of Mathematics **31** (2020), no. 06, 2050046, Publisher: World Scientific Publishing Co.
- [GJL21] Li Gao, Marius Junge, and Haojian Li, *Geometric Approach Towards Complete Logarithmic Sobolev Inequalities*, arXiv:2102.04434 [quant-ph] (2021), arXiv: 2102.04434.
- [GKS76] Vittorio Gorini, Andrzej Kossakowski, and E. C. G. Sudarshan, *Completely positive dynamical semigroups of  $N$ -level systems*, Journal of Mathematical Physics **17** (1976), no. 5, 821–825, Publisher: American Institute of Physics.
- [GR21] Li Gao and Cambyse Rouzé, *Complete entropic inequalities for quantum Markov chains*, arXiv:2102.04146 [quant-ph] (2021), arXiv: 2102.04146.
- [Gro75a] Leonard Gross, *Hypercontractivity and logarithmic Sobolev inequalities for the Clifford-Dirichlet form*, Duke Mathematical Journal **42** (1975), no. 3, 383–396, Publisher: Duke University Press.
- [Gro75b] ———, *Logarithmic Sobolev Inequalities*, American Journal of Mathematics **97** (1975), no. 4, 1061–1083, Publisher: Johns Hopkins University Press.
- [HBY21] Alexander Hahn, Daniel Burgarth, and Kazuya Yuasa, *Unification of Random Dynamical Decoupling and the Quantum Zeno Effect*, arXiv:2112.04242 [quant-ph] (2021), arXiv: 2112.04242.
- [HM18] Aram Harrow and Saeed Mehraban, *Approximate unitary  $t$ -designs by short random quantum circuits using nearest-neighbor and long-range gates*, arXiv:1809.06957 [quant-ph] (2018), arXiv: 1809.06957.
- [HS21] Patrick Hayden and Jonathan Sorce, *On the magnitude of dissipation in open quantum systems*, arXiv:2108.08316 [cond-mat, physics:math-ph, physics:quant-ph] (2021), arXiv: 2108.08316.
- [JLR19] Marius Junge, Nicholas LaRacuate, and Cambyse Rouzé, *Stability of logarithmic Sobolev inequalities under a noncommutative change of measure*, arXiv:1911.08533 [math-ph, physics:quant-ph] (2019), arXiv: 1911.08533.
- [Jon83] V. F. R. Jones, *Index for subfactors*, Inventiones mathematicae **72** (1983), no. 1, 1–25 (en).
- [Kat50] Tosio Kato, *On the Adiabatic Theorem of Quantum Mechanics*, Journal of the Physical Society of Japan **5** (1950), no. 6, 435–439, Publisher: The Physical Society of Japan.
- [Kos84] Hideki Kosaki, *Applications of the complex interpolation method to a von Neumann algebra: Non-commutative  $L_p$ -spaces*, Journal of Functional Analysis **56** (1984), no. 1, 29–78.

- [KT13] Michael J. Kastoryano and Kristan Temme, *Quantum logarithmic Sobolev inequalities and rapid mixing*, Journal of Mathematical Physics **54** (2013), no. 5, 052202, Publisher: American Institute of Physics.
- [LaR21] Nicholas LaRacunte, *Quasi-factorization and Multiplicative Comparison of Subalgebra-Relative Entropy*, arXiv:1912.00983 [quant-ph] (2021), arXiv: 1912.00983.
- [Lin76] G. Lindblad, *On the generators of quantum dynamical semigroups*, Communications in Mathematical Physics **48** (1976), no. 2, 119–130 (en).
- [LSI<sup>+</sup>22] Nicholas LaRacunte, Kaitlin N. Smith, Poolad Imany, Kevin L. Silverman, and Frederic T. Chong, *Short-Range Microwave Networks to Scale Superconducting Quantum Computation*, arXiv:2201.08825 [quant-ph] (2022), arXiv: 2201.08825.
- [MGE12] Easwar Magesan, Jay M. Gambetta, and Joseph Emerson, *Characterizing quantum gates via randomized benchmarking*, Physical Review A **85** (2012), no. 4, 042311, Publisher: American Physical Society.
- [MR21] Tim Möbus and Cambyse Rouzé, *Optimal convergence rate in the quantum Zeno effect for open quantum systems in infinite dimensions*, arXiv:2111.13911 [math-ph, physics:quant-ph] (2021), arXiv: 2111.13911.
- [MS77] B. Misra and E. C. G. Sudarshan, *The Zeno’s paradox in quantum theory*, Journal of Mathematical Physics **18** (1977), no. 4, 756–763, Publisher: American Institute of Physics.
- [MW19] Tim Möbus and Michael M. Wolf, *Quantum Zeno effect generalized*, Journal of Mathematical Physics **60** (2019), no. 5, 052201, Publisher: American Institute of Physics.
- [noa21] *Solving the Lindblad dynamics of a qubit chain — Qiskit Dynamics Solvers 0.2.1 documentation*, 2021, [https://qiskit.org/documentation/dynamics/tutorials/Lindblad\\_dynamics\\_simulation.html](https://qiskit.org/documentation/dynamics/tutorials/Lindblad_dynamics_simulation.html).
- [PP86] Mihai Pimsner and Sorin Popa, *Entropy and index for subfactors*, Annales scientifiques de l’École Normale Supérieure **19** (1986), no. 1, 57–106 (fr).
- [Rob55] Herbert Robbins, *A Remark on Stirling’s Formula*, The American Mathematical Monthly **62** (1955), no. 1, 26–29, Publisher: Mathematical Association of America.
- [SBEP21] John P. T. Stenger, Nicholas T. Bronn, Daniel J. Egger, and David Pekker, *Simulating the dynamics of braiding of Majorana zero modes using an IBM quantum computer*, Physical Review Research **3** (2021), no. 3, 033171, arXiv: 2012.11660.
- [Suz76] Masuo Suzuki, *Generalized Trotter’s formula and systematic approximants of exponential operators and inner derivations with applications to many-body problems*, Communications in Mathematical Physics **51** (1976), no. 2, 183–190 (en).
- [Win16] Andreas Winter, *Tight Uniform Continuity Bounds for Quantum Entropies: Conditional Entropy, Relative Entropy Distance and Energy Constraints*, Communications in Mathematical Physics **347** (2016), no. 1, 291–313 (en).

## APPENDIX A. ADDITIONAL MATH BACKGROUND

**A.1. Distance and Entropy Measures.** We recall the Umegaki relative entropy given by

$$D(\rho\|\sigma) := \text{tr}(\rho \log \rho - \rho \log \sigma) .$$

for two densities  $\rho, \sigma \in \mathcal{D}(\mathcal{H})$ . Beyond tracial settings, the relative entropy has a more general definition via Tomita-Takesaki modular theory. Though many results used in this paper are derived with relative entropy using the natural logarithm, the logarithm base does not matter when comparing ratios of entropies. We will by default denote the logarithm with base 2 for compatibility with the experimental conventions in Section 2.

By  $\rho \geq \sigma$ , we mean that  $\rho$  is greater than  $\sigma$  in the Loewner order:  $\rho - \sigma$  is a non-negative matrix. We say for a pair of quantum channels  $\Phi, \Psi : \mathcal{D}(\mathcal{H}) \rightarrow \mathcal{D}(\mathcal{H})$  that  $\Psi \geq_{cp} \Phi$  iff

$$(\Psi \otimes \hat{1}^B)(\rho) \geq (\Phi \otimes \hat{1}^B)(\rho)$$

for all finite-dimensional auxiliary systems  $B$ . We call this and the associated symbols  $<_{cp}$ ,  $\leq_{cp}$ , and  $>_{cp}$  cp-order relations. Via the Choi-Jamiołkowski isomorphism, a finite-dimensional quantum channel is fully defined by its action on one side of a maximally entangled state between its input space and an auxiliary space of the same dimension. Hence if  $\Phi \geq_{cp} \Psi$ , then  $\Psi = (1 - \epsilon)\Phi + \epsilon\Theta$  for some  $\epsilon \in (0, 1)$  and other channel  $\Theta$ .

We denote the Schatten norms  $\|\cdot\|_p$  for  $p \in [0, \infty]$ . The trace distance is given by

$$d_{tr}(\rho, \sigma) := \frac{1}{2} \|\rho - \sigma\|_1 .$$

In general, for a pair of Banach spaces  $\mathcal{A}$  and  $\mathcal{B}$  with respective norms  $\|\cdot\|_{\mathcal{A}}$  and  $\|\cdot\|_{\mathcal{B}}$ , the  $\mathcal{A} \rightarrow \mathcal{B}$  norm on maps from  $\mathcal{A}$  to  $\mathcal{B}$  is given by

$$\|\Phi\|_{\mathcal{A} \rightarrow \mathcal{B}} := \sup_{\rho \in \mathcal{A}} \frac{\|\Phi(\rho)\|_{\mathcal{B}}}{\|\rho\|_{\mathcal{A}}} .$$

For von Neumann algebras of the same type  $\mathcal{A}$  and  $\mathcal{B}$ , we denote  $\|\Phi\|_{\mathcal{A} \rightarrow \mathcal{B}, cb} := \sup_{\mathcal{C}} \|\Phi \otimes \hat{1}^{\mathcal{C}}\|_{\mathcal{A} \otimes \mathcal{C} \rightarrow \mathcal{B} \otimes \mathcal{C}}$ , where  $\mathcal{C}$  is an extension over von Neumann algebras of the same type as  $\mathcal{A}$  and  $\mathcal{B}$  with a compatible norm in each tensor product. We denote  $\|\Phi\|_{p \rightarrow q, cb} = \|\Phi\|_{\mathcal{A} \rightarrow \mathcal{B}, cb}$  in which  $\|\cdot\|_{\mathcal{A}} = \|\cdot\|_p$  and  $\|\cdot\|_{\mathcal{B}} = \|\cdot\|_q$ . The diamond norm on a map  $\Phi$  is defined as  $\|\Phi\|_{\diamond} := \|\Phi\|_{1 \rightarrow 1, cb}$ . We call a map  $\Phi$  an  $\mathcal{A} \rightarrow \mathcal{B}$  contraction if  $\|\Phi\|_{\mathcal{A} \rightarrow \mathcal{B}} \leq 1$ .

When  $\mathcal{E}$  is the conditional expectation to the fixed point subspace of a Lindbladian with GNS detailed balance,  $\mathcal{E}$  has the following properties:

- (1) As a projector,  $\mathcal{E}$  is idempotent.
- (2)  $\mathcal{E}$  is self-adjoint with respect to the GNS inner product for  $\omega$ .
- (3)  $\mathcal{E}$  has the following bimodule property: for any  $a, b \in \mathcal{N}$  and  $x \in \mathbb{B}(\mathcal{H})$ ,  $\mathcal{E}^*(axb) = a\mathcal{E}^*(x)b$ . Following, for any density  $\rho \in \mathcal{D}(\mathcal{H})$ ,  $\mathcal{E}(a\rho b) = a\mathcal{E}(\rho)b$ .

For the entropy comparison in Equation 16, a concrete bound in [LaR21] establishes that

$$\beta_{c, \zeta} \leq \frac{1}{1 + \zeta(c+1) + 2\zeta^2(c-1)} \left( 1 - 2\zeta(2 + \zeta) \frac{(c-1)^2}{c(\ln c - 1) + 1} - 6\zeta - \zeta^2 \right) .$$

One may also use some of the approximate tensorization estimates from [GR21].

## APPENDIX B. REANALYSIS OF THE GENERALIZED ZENO EFFECT

This Subsection is devoted to a technical reanalysis of the generalized Zeno effect. Rather than spectral properties of the channels involved, we base our estimates on cp-order inequalities and seek comparability with CMLSI and  $\lambda$ -decay.

The bounds derived herein are nonetheless in terms of norms as described in Appendix A. These bounds are in principle very general, requiring only sub-multiplicativity of  $\|\cdot\|_{\mathcal{A}\rightarrow\mathcal{B}}$  in addition to its being a norm. A restriction, however, is that many of the results must assume contractivity of most or all maps involved. The diamond norm is especially convenient in this sense, as channels automatically satisfy this assumption. The diamond norm is however only clearly usable in algebras with a finite trace, which extends it to some but not all infinite-dimensional settings. In principle, one could apply results herein using the Kosaki norms [Kos84] in all von Neumann algebras, but more care would be needed to ensure contractivity of involved maps and in some cases boundedness and analyticity. Since the purpose of this paper is however to understand the relationship between the Zeno effect and mostly finite-dimensional semigroups, we will not be too concerned with technical barriers in non-tracial settings. For infinite-dimensional versions of the Zeno effect, see [BDS21, MR21].

To simplify notation, let

$$F_a^{(m)} := \frac{a^m \exp(a)}{m!} \quad (23)$$

for any scalar  $a > 0$ ,  $k \in \mathbb{N}$ .

**Remark B.1.** For any  $a > 0$  such that  $\exp(a)$  equals its Taylor series,

$$\exp(a) - \sum_{n=0}^k \frac{a^n}{n!} = \sum_{n=k+1}^{\infty} \frac{a^n}{n!} = a^{k+1} \sum_{n=0}^{\infty} \frac{a^n}{(n+k+1)!} \leq \frac{a^{k+1} \exp(a)}{(k+1)!} = F_a^{(k+1)}.$$

**Lemma B.2.** Let  $\mathcal{L}$ , and  $\mathcal{E}$  be respectively a Lindbladian and a map on the same von Neumann algebra. Let  $\mathcal{A}$  be a normed input subspace that is preserved by  $\mathcal{L}$ , and  $\mathcal{B}$  be the normed output space of  $\mathcal{E}$ . Then for any  $t \in \mathbb{R}$

$$\left\| \mathcal{E} \circ \sum_{m=k}^{\infty} \frac{(it)^m}{m!} \mathcal{L}^m \right\|_{\mathcal{A}\rightarrow\mathcal{B},(cb)} \leq F_{\|\mathcal{L}\|_{\mathcal{A},(cb)} t}^{(k)} \|\mathcal{E}\|_{\mathcal{A}\rightarrow\mathcal{B},(cb)}.$$

*Proof.* First, we name a given input  $\rho$  and use the triangle inequality to separate terms.

$$\left\| \mathcal{E} \circ \sum_{m=k}^{\infty} \frac{(it)^m}{m!} \mathcal{L}^m \right\|_{\mathcal{A}\rightarrow\mathcal{B},(cb)} \leq \sum_{m=k}^{\infty} \frac{t^m}{m!} \|\mathcal{E} \circ \mathcal{L}^m\|_{\mathcal{A}\rightarrow\mathcal{B},(cb)}. \quad (24)$$

We then consider each term.

$$\|\mathcal{E} \circ \mathcal{L}^m(\rho)\|_{\mathcal{A}\rightarrow\mathcal{B},(cb)} \leq \|\mathcal{E}\|_{\mathcal{A}\rightarrow\mathcal{B},cb} \|\mathcal{L}^m(\rho)\|_{\mathcal{A},(cb)}.$$

The proof then follows from Remark B.1.  $\square$

**Lemma B.3.** *Let  $(f_m)_{m=1}^k, (g_m)_{m=1}^k$  be families of maps for  $k \in \mathbb{N}$  such that  $f_m \circ f_{m-1}$  and  $g_m \circ g_{m-1}$  are valid compositions. Let  $\omega_l = \prod_{m=1}^l f_m(\rho)$  for input  $\rho$ . Then*

$$\prod_{m=1}^k g_m - \prod_{m=1}^k f_m = \sum_{l=1}^k \left( \prod_{n=l+1}^k g_n \right) (f_l - g_l)(\omega_{l-1}).$$

*Proof.* For one value of  $l$ ,

$$\prod_{n=l+1}^k g_n(\omega_l) - \prod_{n=l}^k g_n(\omega_{l-1}) = \prod_{n=l+1}^k (g_n - g_n)(\omega_{l-1}).$$

The Lemma then follows from induction.  $\square$

**Corollary B.4.** *Let  $(f_m)_{m=1}^k, (g_m)_{m=1}^k$  be families of maps as in Lemma B.3, and further assume that these maps are defined from a normed Banach space to itself. Then*

$$\left\| \prod_{m=1}^k g_m - \prod_{m=1}^k f_m \right\| \leq \sum_{l=0}^{k-1} \left\| \prod_{n=l+1}^k g_n \right\| \|f_l - g_l\|.$$

### B.1. Results for Cp-order Comparable Interruptions.

**Proposition B.5.** *Let  $\mathcal{L}$  and  $\mathcal{E}$  be respectively a Lindbladian and projection to the subspace  $\mathcal{N} \subseteq \mathcal{A}$  defined on Banach space  $\mathcal{A}$  such that  $\exp(-\mathcal{L})$  is equal to its Taylor series. Let  $(t_m)_{m=1}^k$  be a family of values in  $\mathbb{R}^+$ . Let  $t = \sum_m t_m$ . Then*

$$\begin{aligned} & \left\| \prod_{m=1}^k (\mathcal{E} \exp(-\mathcal{L}t_m/k) \mathcal{E}) - \exp(-t\mathcal{E} \circ \mathcal{L} \circ \mathcal{E}) \right\|_{\mathcal{N} \rightarrow \mathcal{N}, (cb)} = O(1/k) \\ & \leq \sum_{m=1}^k \left( \|\mathcal{E}\|_{\mathcal{A} \rightarrow \mathcal{N}, (cb)} F_{t_m}^{(2)} \|\mathcal{L}\|_{\mathcal{A} \rightarrow \mathcal{A}, (cb)}/k + F_{t_m}^{(2)} \|\mathcal{E}\mathcal{L}\mathcal{E}\|_{\mathcal{N} \rightarrow \mathcal{N}, (cb)}/k \right) \left\| \exp\left(-\frac{\mathcal{E}\mathcal{L}\mathcal{E}}{k} \sum_{n=m+1}^k t_n\right) \right\|_{\mathcal{N} \rightarrow \mathcal{N}, (cb)}. \end{aligned}$$

*Proof.* First, we show for one value of “ $t$ ” that

$$\|\mathcal{E} R_{itH} \mathcal{E}(\rho) - \exp(-t\mathcal{E} \circ \mathcal{L} \circ \mathcal{E}) \mathcal{E}\|_{\mathcal{N} \rightarrow \mathcal{N}, (cb)} \leq (F_{\|\mathcal{L}\|_{\mathcal{N} \rightarrow \mathcal{A}} t}^{(2)} + F_{\|\mathcal{E} \circ \mathcal{L} \circ \mathcal{E}\|_{\mathcal{N} \rightarrow \mathcal{A}, (cb)} t}^{(2)}). \quad (25)$$

For any input  $\rho$ , one may Taylor expand

$$(\mathcal{E} \circ \exp(-\mathcal{L}t) \circ \mathcal{E})(\rho) = \mathcal{E}(\rho) - t\mathcal{E}(\mathcal{L}(\mathcal{E}(\rho))) + \mathcal{E}\left(\sum_{m=2}^{\infty} \frac{(-t)^m}{m!} \mathcal{L}^m(\mathcal{E}(\rho))\right) \quad (26)$$

The terms up to first order in  $t$  match those of  $\exp(-t\mathcal{E} \circ \mathcal{L} \circ \mathcal{E})$ . Via the triangle inequality and idempotence of  $\mathcal{L}$ , what remains is to bound the distance of higher order terms,

$$\left\| \mathcal{E}\left(\sum_{m=2}^{\infty} \frac{(-t)^m}{m!} \mathcal{L}^m(\mathcal{E}(\rho))\right) - \sum_{m=2}^{\infty} \frac{(-t)^m}{m!} (\mathcal{E} \circ \mathcal{L} \circ \mathcal{E})^m(\mathcal{E}(\rho)) \right\|_{\mathcal{N} \rightarrow \mathcal{N}, (cb)}.$$

We apply Lemma B.2 to each higher-order sequence individually, using the triangle inequality to separate them. This step completes the proof of Equation (25).

We then apply Corollary B.4. The fact that  $\exp(a)\exp(b) = \exp(a+b)$  whenever  $[a, b] = 0$  completes the Proposition.  $\square$



Proposition B.5 simplifies when bounding the diamond norm, because quantum channels are contractions. Hence

$$\left\| \prod_{m=1}^k (\mathcal{E} \exp(-\mathcal{L}t_m/k) \mathcal{E}) - \exp(-t\mathcal{E} \circ \mathcal{L} \circ \mathcal{E}) \circ \mathcal{E} \right\|_{\diamond} \leq \sum_{m=1}^k (F_{t_m \|\mathcal{L}\|_{\diamond}/k}^{(2)} + F_{t_m \|\mathcal{E}\mathcal{L}\mathcal{E}\|_{\diamond}/k}^{(2)}). \quad (27)$$

Proposition B.5 yields additional simplifications when  $\mathcal{L}$  has the form of a Hamiltonian:

**Remark B.6.** *When  $\mathcal{E}$  is a conditional expectation and  $\mathcal{L} = i[H, \cdot]$  for some Hamiltonian  $H$ , the bimodule property of conditional expectations implies that for any input  $\rho$ ,*

$$\mathcal{E}(i[H, \mathcal{E}_0(\rho)]) = i\mathcal{E}(H\mathcal{E}(\rho)) - i\mathcal{E}(\mathcal{E}(\rho)H) = i[\mathcal{E}(H), \mathcal{E}(\rho)]. \quad (28)$$

**Lemma B.7.** *For any  $p$  such that  $\|\cdot\|_{p \rightarrow p}$  is a norm and  $\|\cdot\|_p$  obeys Hölder's inequality,*

$$\|[H, \cdot]^m\|_{p \rightarrow q, (cb)} \leq 2^m \|H\|_{\infty}^m \sup_{\rho} \|\rho\|_q / \|\rho\|_p$$

*Proof.* For Hamiltonians, we use the fact that  $[H, \cdot]^m(\rho)$  generates  $2^m$  terms on any density  $\rho$ , each of which contains  $m$  powers of  $H$  and one of  $\rho$ . Using Hölder's inequality and its inductive generalization,

$$\|H^k \rho H^{m-k}\|_p \leq \|H^k\|_{\infty} \|\rho H^{m-k}\|_p \leq \|H^k\|_{\infty} \|\rho\|_p \|H^{m-k}\|_{\infty} \leq \|\rho\|_p \|H\|_{\infty}^m$$

for any integer  $k$  such that  $0 \leq k \leq m$ . Hence

$$\|[H, \cdot]^m\|_{p \rightarrow p} = \sup_{\rho} \|[H, \cdot]^m(\rho)\|_p / \|\rho\|_p \leq 2^m \|H\|_{\infty}^m.$$

To conclude the Lemma, we return to Equation (24) and re-assemble the exponential series, using Remark B.1.  $\square$

Our next step is to generalize Proposition B.5 from a projection  $\mathcal{E}$  to a quantum channels  $\Phi$  such that  $\Phi \geq_{cp} (1 - \epsilon)\mathcal{E}$  for some  $\epsilon \in [0, 1)$ . First, we prove a replacement for [MR21, Lemma 5.2], which replaces a general contraction by its fixed point projector. Our replacement consists of several Lemmas.

**Lemma B.8.** *Let  $\Psi_1, \dots, \Psi_w$  be quantum channels such that  $\mathcal{E}\Psi_m = \Psi_m\mathcal{E} = \mathcal{E}$  for each  $m \in 1 \dots w$ , let  $R := \exp(-\mathcal{L}t/k)$ , and assume  $\|\Psi_m\|_{\mathcal{N} \rightarrow \mathcal{N}, (cb)} \leq a$  for some  $a \in \mathbb{R}^+$  and all  $m \in 1 \dots w$ . Let  $\mathcal{A}$  be the normed input Banach space. Then*

$$\begin{aligned} & \left\| \mathcal{E} \prod_{m=1}^w (\Psi_m R) \mathcal{E} - \mathcal{E} R^w \mathcal{E} \right\|_{\mathcal{A} \rightarrow \mathcal{B}, (cb)} \\ & \leq \|\mathcal{E}\|_{\mathcal{A} \rightarrow \mathcal{B}, (cb)} \left( (a^w + 1) F_{tw \|\mathcal{L}\|_{\mathcal{N} \rightarrow \mathcal{N}, (cb)}/k}^{(2)} + w a^w F_{t \|\mathcal{L}\|_{\mathcal{N} \rightarrow \mathcal{N}, (cb)}/k}^{(2)} \right), \end{aligned} \quad (29)$$

where we are free to choose  $\mathcal{N} = \mathcal{A}$  or  $\mathcal{N} = \mathcal{B}$  assuming  $\|\mathcal{E}\|_{\mathcal{N} \rightarrow \mathcal{N}, (cb)} \leq 1$  and  $\|R\|_{\mathcal{N} \rightarrow \mathcal{N}, (cb)} \leq 1$ .

Under the assumption that channels involved are  $\mathcal{A} \rightarrow \mathcal{A}$  norm contractions,

$$\left\| \mathcal{E} \prod_{m=1}^w (\Psi_m R) \mathcal{E} - \mathcal{E} R^w \mathcal{E} \right\|_{\mathcal{A} \rightarrow \mathcal{A}, (cb)} \leq \frac{1}{2} \left( \frac{t \|\mathcal{L}\|_{\mathcal{A} \rightarrow \mathcal{A}, (cb)}}{k} \right)^2 \exp(tw \|\mathcal{L}\|_{\mathcal{A} \rightarrow \mathcal{A}, (cb)}/k) (2w^2 + w). \quad (30)$$

*Proof.* Via Taylor expansion and the assumption that  $\mathcal{E}\Psi = \Psi\mathcal{E} = \mathcal{E}$ ,

$$\begin{aligned} \mathcal{E} \prod_{n=1}^w (\Psi_n R) \mathcal{E} &= \mathcal{E} - \frac{wt}{k} \mathcal{E} \sum_{m=0}^w \Psi_1 \dots \Psi_m \mathcal{L} \Psi_m \dots \Psi_w \circ \mathcal{E} + h.o.t.(1) \\ &= \mathcal{E} - \frac{wt}{k} \mathcal{E} \sum_{m=0}^w \mathcal{L} \circ \mathcal{E} + h.o.t.(1). \end{aligned} \quad (31)$$

For comparison,

$$\mathcal{E} R^w \mathcal{E} = \mathcal{E} - \frac{wt}{k} \mathcal{E} \sum_{m=0}^w \mathcal{L} \circ \mathcal{E} + h.o.t.(2). \quad (32)$$

As in Proposition B.5, the first order terms of compared quantities match. The second set of higher-order terms is bounded simply via Lemma B.2. Hence

$$\|h.o.t.(2)\| \leq \|R^w - (1 - \mathcal{L}tw/k)\| \leq F_{tw\|\mathcal{L}\|/k}^{(2)}. \quad (33)$$

The terms of  $h.o.t.(1)$  are more complex, as they may combine multiple orders of Taylor expansion. To simplify the expression, we first estimate each  $R$  factor by the linear order  $1 - \mathcal{L}t/k$ , which yields the same estimate as in Equation (33) for  $w = 1$  and with a factor of  $a^w$ .

Analyzing the remaining expression combinatorially,

$$\begin{aligned} &\left\| \mathcal{E} \left( \prod_{n=1}^w (\Psi_n (1 - \mathcal{L}t/k)) - (1 - \mathcal{L}tw/k) \right) \mathcal{E} \right\|_{\mathcal{A} \rightarrow \mathcal{B}, (cb)} \\ &\leq \|\mathcal{E}\|_{\mathcal{A} \rightarrow \mathcal{B}, (cb)} a^w \sum_{m=2}^w \left(\frac{t}{k}\right)^m \binom{w}{m} \|\mathcal{L}\|_{\mathcal{N} \rightarrow \mathcal{N}, (cb)}^m. \end{aligned} \quad (34)$$

Since ( $w$  choose  $m$ )  $< w^m/m!$ , the sum is upper bounded as

$$\sum_{m=2}^w \left(\frac{t}{k}\right)^m \binom{w}{m} \|\mathcal{L}\|^m \leq \sum_{m=2}^w \frac{1}{m!} \left(\frac{tw}{k} \|\mathcal{L}\|\right)^m \leq F_{tw\|\mathcal{L}\|/k}^{(2)}. \quad (35)$$

For the last inequality, we used Lemma B.2 and the fact that the finite sum is upper bounded by a sum going to infinity. Combining the contributions from Equations (33)-(35), we arrive at the Lemma.  $\square$

**Lemma B.9.** *Let  $X$  be an IID binary random variable with outcomes 0 and 1, 1 having probability  $\epsilon$ . Let  $f : \cup_{k \in \mathbb{N}} \{0, 1\}^k \rightarrow \mathbb{R}^+$  be a function that depends only and monotonically on the number of sequences of successive 1s of each length within its input string. Let  $p_{nb}[m, \epsilon] : \cup_{k \in \mathbb{N}} \{0, 1\}^k \rightarrow [0, 1]$  give the probability of each binary sequence if constructed by repeatedly drawing bits from  $X$  until encountering  $m$  0s. Then*

$$\sum_{s \in X^k} f(s) \leq \sum_{s \in \cup_{l \in \mathbb{N}} \{0, 1\}^l} \left( p_{nb}[k(1 - \epsilon) + \sqrt{k \ln k}, \epsilon](s) f(s) + \frac{1}{k^2} p_{nb}[k, \epsilon](s) f(s) \right).$$

For a simple overcounting, one may consider a scenario in which starts at each of  $k$  positions, generating 1s until encountering a 0. The advantage of this simple model is that we reduce the problem to  $k$  copies of a geometric series. The disadvantage is that for a sequence of expected

length  $k(1 + \langle w \rangle)$ , where  $\langle w \rangle$  is the expected length of a cluster of 1s, this method potentially overcounts by a substantial factor when  $\epsilon$  is not small. To better control the overcount, we apply concentration inequalities to separate the rare events in which the number of these clusters substantially exceeds  $k/\langle w \rangle$ . We note that the sum  $\sum_{s \in \cup_{l \in \mathbb{N}} \{0,1\}^l} p_{nb}[k, \epsilon](s) f(s)$  is equivalent to summing over all possible geometrically distributed window lengths on  $k$  trials.

*Proof.* After each 1, the number,  $w$ , of 0s before the next 1 is approximately distributed geometrically as  $p(w) = (1 - \epsilon)\epsilon^w$ . There is a small overcount due to value of  $w$  that exceed  $k$ . This geometric distribution has mean  $\langle w \rangle = \epsilon/(1 - \epsilon)$  and variance  $\epsilon/(1 - \epsilon)^2$ .

While one could consider  $k$  such sequences, such would more substantially overestimate the number of total factors as roughly  $k(1 + \langle w \rangle)$ . For any  $l \in \mathbb{N}$ ,  $p(w \geq l) = (1 - \epsilon) \sum_{w \geq l} \epsilon^w = \epsilon^l$ . Conversely,  $p(w < l) = 1 - \epsilon^l$ . For  $\alpha \in [0, 1]$ , we aim to upper bound the probability that after encountering  $\alpha k$  clusters of  $\Psi R$  factors, we will have not yet encountered  $k$  total terms. As a sum of geometric distributions, the total probability of obtaining at most  $k$  total factors among  $\alpha k \mathcal{E}_0 R$  factors is given by a cumulative negative binomial distribution. Equivalently, this probability is given by sum of binomial distributions to obtain between  $(1 - \alpha)k$  and  $k$  “failures” in  $k$  trials with “failure” probability  $\epsilon$ . Assuming that  $\alpha > 1 - \epsilon$ , the probability of not obtaining at least  $k$  “failures” admits the Chernoff bound,

$$p(\# \text{ failures} < (1 - \alpha)k | k \text{ trials}) \leq \exp(-kD(1 - \alpha|\epsilon)), \quad (36)$$

where  $D(\cdot|\cdot)$  is the binary relative entropy. In the event that  $\alpha k$  attempts do not suffice to obtain  $k$  total factors, we must continue to add factors to avoid a potential underestimate.

One remaining step is to find a reasonable choice of  $\alpha$ . Via Pinsker’s inequality, we may reduce the Chernoff bound to the simpler Hoeffding bound,

$$\exp(-kD(1 - \alpha|\epsilon)) \leq \exp(-2k(\epsilon + \alpha - 1)^2). \quad (37)$$

Differentiating the Hoeffding bound, we find the approximate condition,

$$1 - 2k(\epsilon + \alpha - 1) \exp(-2k(\epsilon + \alpha - 1)^2) = 0. \quad (38)$$

As this condition remains non-trivial, we make the simplifying choice  $\alpha = 1 - \epsilon + \sqrt{\ln k/k}$ .  $\square$

Combining the previous two Lemmas,

**Lemma B.10.** *Let  $(\Phi_m)$  be quantum channels with  $\epsilon \in (0, 1)$  and projector  $\mathcal{E}$  such that  $\Phi_m \geq_{cp} (1 - \epsilon)\mathcal{E}$  for all  $m \in \mathbb{N}$ . Let  $\mathcal{L}$  be a Lindbladian on the same space. Assume that  $\Phi$ ,  $\mathcal{E}$ , and  $\exp(-\mathcal{L}t/k)$  are norm contractions for all  $t \in \mathbb{R}^+$ . Further assume sufficiently large  $k > 1$  that  $t\|\mathcal{L}\|/k \leq \ln(1/\epsilon)$ . Then*

$$\begin{aligned} & \left\| \prod_{m=1}^k \left( \Phi_m \circ \exp(-\mathcal{L}t/k) \right) - \mathcal{E} \circ (((1 - \epsilon)\mathcal{E} + \epsilon\hat{1}) \circ \exp(-\mathcal{L}t/k)) \circ \mathcal{E} \right\| \\ & \leq \frac{3\epsilon(1 - \epsilon + 2\sqrt{(\ln k)/k})kF_c^{(2)}}{(1 - \epsilon \exp(c))^2} + \frac{4\epsilon F_{t\|\mathcal{L}\|/k}^{(1)}}{(1 - \epsilon)^2} = O(\epsilon/k), \end{aligned} \quad (39)$$

where  $c := t\|\mathcal{L}\|/k$ .

The intuition for this Lemma is that when  $\Phi = (1 - \epsilon)\mathcal{E} + \epsilon\Psi$ , we may treat each occurrence as a binary random variable and sum over sequences containing either  $\mathcal{E}$  or  $\Psi$  at each location. There are typically not too many powers of  $\Psi R_{-\exp(-\mathcal{L}t/k)}$  between successive powers of  $\mathcal{E}$ .

*Proof.* First,  $\Phi \geq_{cp} (1 - \epsilon)\mathcal{E}$  implies that  $\Phi = (1 - \epsilon)\mathcal{E} + \epsilon\Psi$  as one may check via the Choi-Jamiolkowski isomorphism. For simplicity of notation, let  $R := \exp(-\mathcal{L}t/k)$ . We will henceforth consider  $k$ -fold sequences in the set  $\otimes_{m=1}^k \{R\mathcal{E}, R\Psi_m\}$ .

We now consider a model in which we begin counting the norm cost of replacing individual windows, optionally stopping as soon as  $k$  total factors appear. As shown via Lemma B.9, we can usually stop after  $\alpha k$  windows as long as  $\alpha > 1 - \epsilon$ . In these cases, we average the bound in Lemma (B.8) over possible window lengths and multiply by  $\alpha k$ . We use the simplified form of Equation (30). To simplify further, we use the well-known formula for linearly and quadratically weighted geometric series to obtain that

$$\sum_{w=1}^k b^w w(1 + 2w) \leq \frac{3b}{(1 - b)^2} \quad (40)$$

for any  $b \in (0, 1)$ . Here we set  $b = \epsilon \exp(t\|\mathcal{L}\|/k)$ . Returning to Equation (30), using the Chernoff bound as in Equation (36), and accounting for the  $(1 - \epsilon)k$ -fold approximate term number,

$$\|(\Phi \circ \exp(-\mathcal{L}t/k))^k - (\mathcal{E} \circ \exp(-\mathcal{L}tm/k))^k \mathcal{E}\| \leq (\alpha + \exp(-kD(1 - \alpha\|\epsilon\|))) \frac{t^2 \|\mathcal{L}\|^2}{k} \frac{3b}{(1 - b)^2} \quad (41)$$

for any  $\alpha < 1 - \epsilon$ . This bound nearly completes the Lemma, yielding with the simplifications in Lemma B.9 that

$$\|(\Phi \circ \exp(-\mathcal{L}t/k))^k - (\mathcal{E} \circ \exp(-\mathcal{L}tm/k))^k \mathcal{E}\| \leq \frac{(1 - \epsilon + 2\sqrt{\ln k/k})t^2 \|\mathcal{L}\|^2 3b}{k(1 - b)^2}, \quad (42)$$

where we absorb the  $1/k^2$  correction into the factor of 2 multiplying  $\sqrt{\ln k/k}$ . The final step is to account for the fact that the first and last factors may not be sandwiched between powers of  $\mathcal{E}$ , so Lemma B.8 may not hold for them. Since we need not contend with  $k$ -fold repetition in this situation, we may directly apply the commutator between  $\Psi$  and  $R$ , noting that  $\|[\Psi, R]\| \leq 2F_{t\|\mathcal{L}\|/k}^{(1)}$  by Lemma B.2. The number of such terms is potentially quadratic in the first and last window length, which after summing these distributions yields an upper bound of  $\epsilon/(1 - \epsilon)^2$ . Via the triangle inequality, we add these terms to the final bound.  $\square$

**Corollary B.11.** *Let  $\mathcal{E}$  be a projector to subspace  $\mathcal{N}$  and  $\mathcal{L}$  a Lindbladian. Then for  $\epsilon \in [0, 1)$ ,*

$$\begin{aligned} & \|\mathcal{E} \circ (((1 - \epsilon)\mathcal{E} + \epsilon\hat{1}) \circ \exp(-\mathcal{L}t/k))^k \circ \mathcal{E} - \exp(-\mathcal{E}\mathcal{L}\mathcal{E}t) \circ \mathcal{E}\| \\ & \leq k(F_{t\|\mathcal{L}\|/k}^{(2)} + F_{t\|\mathcal{E}\mathcal{L}\mathcal{E}\|/k}^{(2)}) \frac{(1 - \epsilon + 2\sqrt{(\ln k)/k})(1 + 2\epsilon \exp(t\|\mathcal{L}\|/k))}{(1 - \epsilon \exp(t\|\mathcal{L}\|/k))^2} = O(1/k). \end{aligned} \quad (43)$$

*Proof.* Recalling Proposition B.5, let  $(t_m)_{m=1}^k$  be a family of values in  $\mathbb{R}^+$  such that  $t = \sum_m t_m$ . Then

$$\left\| \prod_{m=1}^k (\mathcal{E} \exp(-\mathcal{L}t_m/k) \mathcal{E}) - \exp(-t\mathcal{E} \circ \mathcal{L} \circ \mathcal{E}) \right\| \leq \sum_{m=1}^k (F_{t_m \|\mathcal{L}\|_{q \rightarrow q}/k}^{(2)} + F_{t_m \|\mathcal{E}\mathcal{L}\mathcal{E}\|/k}^{(2)})$$

under the assumptions of this Lemma. As in the proof of Lemma B.10, we will approximate the distribution of possible sets of  $\{t_m\}$  as  $(1-\epsilon)k$  concatenated windows of geometrically distributed length  $w$ , each surrounded by a pair of  $\mathcal{E}$  factors. We note however that the minimum window length is not 0 in this case, but 1 - adjacent factors of  $\mathcal{E}$  will still have a factor of  $\exp(-\mathcal{L}t_m/k)$  in between. We can still apply Lemma B.9. since typically the number of windows scales like  $1-\epsilon$ . Each factor of  $\hat{1}$  increases the window size by 1. For one such window, let  $b = \epsilon \exp(t\|\mathcal{L}\|/k)$ . Then we approximate the geometric series,

$$\sum_{w=0}^k b^w (1+w^2) \leq \frac{1+2b}{(1-b)^2}.$$

For the full bound,

$$\begin{aligned} & \|\mathcal{E}(((1-\epsilon)\mathcal{E} + \epsilon\hat{1}) \exp(-\mathcal{L}t/k))^k \mathcal{E} - \exp(-\mathcal{E}\mathcal{L}\mathcal{E}t)\mathcal{E}\| \\ & \leq \frac{(1-\epsilon + 2\sqrt{(\ln k)/k})t^2 \|\mathcal{L}\|^2}{k} \frac{1+2b}{(1-b)^2}, \end{aligned} \quad (44)$$

absorbing the  $O(1/k^2)$  correction term from Lemma B.9 into the factor of 2 multiplying  $\sqrt{\ln k/k}$ . The Corollary then follows from expanding  $b$ .  $\square$

The culmination of this Section so far is analogous to [MR21, Theorem 3.1]:

**Theorem B.12.** *Let  $(\Phi_m)$  be quantum channels with  $\epsilon \in (0, 1)$  and projector  $\mathcal{E}$  such that  $\Phi_m \geq_{cp} (1-\epsilon)\mathcal{E}$  for all  $m \in \mathbb{N}$ . Let  $\mathcal{L}$  be a Lindbladian on the same space. Assume that  $\Phi$ ,  $\mathcal{E}$ , and  $\exp(-\mathcal{L}t/k)$  are norm contractions for all  $t \in \mathbb{R}^+$ . Further assume sufficiently large  $k > 1$  that  $t\|\mathcal{L}\|/k \leq \ln(1/\epsilon)$ . Then*

$$\begin{aligned} & \left\| \prod_{m=1}^k (\Phi_m \circ \exp(-\mathcal{L}t/k)) - \exp(-\mathcal{E}\mathcal{L}\mathcal{E}t) \circ \mathcal{E} \right\| \\ & \leq \frac{k(1-\epsilon + 2\sqrt{(\ln k)/k})}{(1-b)^2} \left( F_{t\|\mathcal{E}\mathcal{L}\mathcal{E}\|/k}^{(2)}(1+2b) + F_{t\|\mathcal{L}\|/k}^{(2)}(1+5b) \right) + \frac{4\epsilon F_{t\|\mathcal{L}\|/k}^{(1)}}{(1-\epsilon)^2}, \end{aligned}$$

where  $b = \epsilon \exp(t\|\mathcal{L}\|/k)$ .

*Proof.* The Theorem follows from using the triangle inequality to combine Lemma B.10 with Corollary B.11.  $\square$

We note that  $\epsilon$  is not necessarily a small parameter. If however one restricts to the regime of small  $\epsilon$ , then still assuming that  $2\sqrt{(\ln k)/k}$ , one may simplify the bound further to

$$\left\| \prod_{m=1}^k \left( \Phi_m \circ \exp(-\mathcal{L}t/k) \right) - \exp(-\mathcal{E}\mathcal{L}\mathcal{E}t) \circ \mathcal{E} \right\| \leq \frac{t^2 \|\mathcal{L}\|^2 (1 + 7b/2) + t \|\mathcal{L}\|_{q \rightarrow q} b}{k(1-b)^2}. \quad (45)$$

Since  $b < 1$ , we can even further simplify to

$$\left\| \prod_{m=1}^k \left( \Phi_m \circ \exp(-\mathcal{L}t/k) \right) - \exp(-\mathcal{E}\mathcal{L}\mathcal{E}t) \circ \mathcal{E} \right\|_{p \rightarrow p} \leq \frac{9t^2 \|\mathcal{L}\|^2 / 2 + t \|\mathcal{L}\|}{k(1-b)^2}. \quad (46)$$

We note however that when  $\epsilon = 0$ , Theorem B.12 recovers bound of Proposition B.5 up to leading order in  $1/k$ . Compared with Theorem B.19, Theorem B.12 is more specific but obtains a better dependence on  $t\|\mathcal{L}\|$ .

**B.2. Results for Maps Converging to Fixed Points.** Here we show Zeno-like effects for both discrete channels compositions and Lindbladian-generated semigroups that converge toward a fixed point projector  $\mathcal{E}$ .

**Lemma B.13.** *Let  $(\Phi_m)_{m=1}^k$  be a family of bounded maps on Banach space  $\mathcal{A}$ . Let  $\mathcal{L}$  be a bounded Lindbladian. Let  $t_1, \dots, t_k \in \mathbb{R}^+$ . Then*

$$\left\| \prod_{m=1}^k (\Phi_m \circ e^{-\mathcal{L}t_m}) - \prod_{m=1}^k (\Phi_m \circ (1 - \mathcal{L}t_m)) \right\| \leq \sum_{r=1}^k \left\| \prod_{m=r+1}^k \Phi_m e^{-\mathcal{L}t_m/k} \right\| F_{\|\mathcal{L}\|t_r}^{(2)}.$$

*Proof.* As in much of this Section, the Lemma follows from noting that  $(1 - \mathcal{L}t)$  is the 1st order Taylor expansion of  $e^{-\mathcal{L}t}$  for any  $t \in \mathbb{R}^+$ , so

$$\|e^{-\mathcal{L}t_m} - (1 - \mathcal{L}t_m)\| \leq F_{\|\mathcal{L}\|t_m}^{(2)}$$

for each  $m \in 1 \dots k$ . Corollary B.4 completes the Lemma.  $\square$

Subsequent Lemmas require some combinatoric notation. For  $m < k \in \mathbb{N}$ , let  $WS(m, k) = \{W : 1 \dots m \rightarrow 1 \dots k\}$  denote the set of partitions of  $k$  into  $m$  contiguous, ordered subsets. In particular,  $W(j)$  denotes a contiguous sequence of indices for  $j \in 1 \dots m$ . As an example, we might take  $(1 \mapsto [1, 2], 2 \mapsto [3], 3 \mapsto [4, 5]) \in WS(3, 5)$ . Let  $|W(j)|$  denote the number of indices in  $W(j)$ , which we will refer to as its length. For any  $n \leq k$ , let  $WS(m, k, n) \subseteq WS(m, k)$  denote the subset of partitions such that  $|W(j)| \geq n$  for all  $j \in 1 \dots m$ . Note that  $WS(m, k, n)$  is the empty set whenever  $n > k/m$ . By  $W(j)[l]$  we denote the  $l$ th index in  $W(j)$  for  $l \in 1 \dots m$ .

**Lemma B.14.** *Let  $(\Phi_m)_{m=1}^k$  be a family contractions on a Banach space for any  $k \in \mathbb{N}$ . Let  $\mathcal{L}$  be a bounded Lindbladian such that  $e^{-\mathcal{L}t}$  is also contractive for all  $t \in \mathbb{R}^+$ . Then for any*

$\alpha : \mathbb{N} \rightarrow (1/k, 1)$  and  $n \in 1 \dots k$ ,

$$\begin{aligned} & \left\| \prod_{m=1}^k \left( \Phi_m \left( 1 - \frac{\mathcal{L}}{k} \right) \right) - \sum_{m=0}^n \frac{(-1)^m}{k^m} \sum_W \prod_{j=1}^m (\Phi_{W(j)} \mathcal{L}) \Phi_{W(m+1)} \right\| \\ & \leq \sum_{m=1}^n \frac{\alpha(m)m \|\mathcal{L}\|^m}{(1-m)!} + \sum_{m=n+1}^k \frac{\|\mathcal{L}\|^m}{m!}, \end{aligned} \quad (47)$$

where  $\Phi_{W(j)} = \Phi_{W(j)[|W(j)|, k]} \circ \dots \circ \Phi_{W(j)[1, k]}$ , and the sum over  $W$  is within the set  $WS(m+1, k, \alpha(m)k)$ .

*Proof.* For convenience of notation, let the norm distance in this Lemma be denoted  $\Delta$ .

The first step is the binomial expansion,

$$(\Phi_m(1 - \mathcal{L}/k))^k = \sum_{m=0}^k \frac{(-1)^m}{k^m} \sum_{W \in WS(m+1, k)} \left( \prod_{j=1}^m (\Phi_{W(j)} \mathcal{L}) \right) \Phi_{W(m+1)s}. \quad (48)$$

Our next step will be to match this against the second term the norm distance  $\Delta$ . We see that the expression in Equation (48) is the same as that in the desired term, except that the latter sums over  $WS(m+1, k, \alpha(m)k)$  instead of over  $WS(m+1, k)$ . Hence we must bound the number and magnitude of terms containing short partitions. We observe that the number of such partitions in is upper-bounded by  $(k \text{ choose } m-1) \times (2 \lceil \alpha(m)k \rceil \text{ choose } 1)/2$ , since we can consider first placing  $m-1$  partition boundaries within  $k$  locations, then choose a final partition boundary that is no more than  $\alpha(m)k$  indices away from one of the  $m-1$  original boundaries or from first or last index. The divisor of 2 arises from the invariance under exchange between the final boundary and its close neighbor. This bound is an overcount, since the first  $m-1$  placements might already contain a one or more partitions that are too small. We will ignore this overcounting, since for  $k/m \gg \alpha(m)k$ , it is not expected to contribute much. We thereby find that

$$\Delta \leq \sum_{m=0}^k \frac{\|\mathcal{L}\|^m}{k^m} \binom{k}{m-1} \lceil \alpha(m)mk \rceil.$$

It is easy to see that  $(k \text{ choose } m-1) \leq k(k-1)^{m-2}/(m-1)!$ . We then observe that  $(k-1)/k \leq k/(k+1)$  and that  $\lceil \alpha(m)mk \rceil \leq \alpha(m)m(k+1)$ . Hence

$$\frac{k(k-1)^{m-2} \lceil \alpha(m)mk \rceil}{k^m (m-1)!} \leq \frac{\alpha(m)m}{(1-m)!}$$

We then handle separately the terms with  $m > n$ . Returning to Equation (48), we apply the coarse bound that the cardinality  $|WS(m+1, k)| \leq (k \text{ choose } m) \leq k^m/m!$ . Hence

$$\left\| \sum_{m=n+1}^k \frac{(-1)^m}{k^m} \sum_{W \in WS(m+1, k)} \prod_{j=1}^m (\Phi_{W(j)} \mathcal{L}) \Phi_{W(m+1)} \right\| \leq \sum_{m=n+1}^k \frac{\|\mathcal{L}\|^m}{m!}.$$

□

**Lemma B.15.** *Let  $\Phi_m$  and  $\mathcal{L}$  be as in Lemma B.14 with the additional assumption that for given  $r \in \mathbb{N}$  and  $\gamma \in \mathbb{R}^+$ ,  $\Phi_{W(j)} \geq_{cp} (1 - \epsilon)\mathcal{E}$  whenever  $|W(j)| \geq k/\gamma$ . Then*

$$\left\| \sum_{m=0}^n \frac{(-1)^m}{k^m} \sum_W \prod_{j=1}^m (\Phi_{W(j)} \mathcal{L}) \Phi_{W(m+1)} - \sum_{m=0}^k \frac{(-\mathcal{E}\mathcal{L}\mathcal{E})^m}{k^m} \right\| \leq \epsilon^{\lfloor \gamma/r \rfloor} \exp(\|\mathcal{L}\|) + \sum_{m=r}^k \frac{\|\mathcal{L}\|^m}{(m-1)!}.$$

*Proof.* We first consider the terms for individual values of  $m$ , rewriting

$$\sum_W \prod_{j=1}^m (\Phi_{W(j)} \mathcal{L}) \Phi_{W(m+1)} = \sum_W \prod_{j=1}^m (((1 - \epsilon_m)\mathcal{E} + \epsilon_m \Psi_{W(j)}) \mathcal{L}) ((1 - \epsilon_m)\mathcal{E} + \epsilon_m \Psi_{W(m+1)})$$

for some maps  $\{\Psi_{W(j)} : j = 1 \dots m+1\}$  such that  $\mathcal{E}\Psi_{W(j)} = \Psi_{W(j)}\mathcal{E} = \mathcal{E}$ . Here  $W \in WS(m+1, k, \lfloor k/m \rfloor)$ , and  $\epsilon_m = \epsilon^{\lfloor \gamma/m \rfloor}$ . We begin by estimating the distance

$$\left\| \prod_{j=1}^m (((1 - \epsilon_m)\mathcal{E} + \epsilon_m \Psi_{W(j)}) \mathcal{L}) ((1 - \epsilon_m)\mathcal{E} + \epsilon_m \Psi_{W(m+1)}) - (\mathcal{E}\mathcal{L}\mathcal{E})^m \right\| \leq \|\mathcal{L}\|^m (1 - (1 - \epsilon^{\lfloor \gamma/r \rfloor})^m)$$

for a single value of  $W$ . This bound follows from the number of  $\mathcal{E}$  vs.  $\Psi_{W(j)}$  being binomially distributed in the first term after expanding, since the compared expressions match when the former contains only  $\mathcal{E}$  and  $\mathcal{L}$  factors. Via Bernoulli's inequality, we simplify  $(1 - (1 - \epsilon^{\lfloor \gamma/m \rfloor})^m) \leq m\epsilon^{\lfloor \gamma/m \rfloor}$ . Hence

$$\begin{aligned} & \left\| \sum_{m=0}^n \frac{1}{k^m} \sum_W \prod_{j=1}^m (((1 - \epsilon_m)\mathcal{E} + \epsilon_m \Psi_{W(j)}) \mathcal{L}) ((1 - \epsilon_m)\mathcal{E} + \epsilon_m \Psi_{W(m+1)}) - (\mathcal{E}\mathcal{L}\mathcal{E})^m \right\| \\ & \leq \sum_{m=0}^n \frac{1}{k^m} \binom{k}{m} \|\mathcal{L}\|^m m \epsilon^{\lfloor \gamma/m \rfloor} \leq \sum_{m=0}^n \frac{\|\mathcal{L}\|^m}{m!} m \epsilon^{\lfloor \gamma/m \rfloor}. \end{aligned} \quad (49)$$

The final inequality follows from recalling that  $\binom{k}{m} \leq k^m/m!$ . Then

$$\sum_{m=0}^n \frac{\|\mathcal{L}\|^m}{m!} m \epsilon^{\lfloor \gamma/m \rfloor} \leq \sum_{m=0}^r \frac{\|\mathcal{L}\|^m}{m!} m \epsilon^{\lfloor \gamma/r \rfloor} + \sum_{m=r}^k \frac{\|\mathcal{L}\|^m}{(m-1)!}.$$

For an overestimate,  $\epsilon^{\lfloor \gamma/m \rfloor} \leq \epsilon^{\lfloor \gamma/r \rfloor}$  for all  $m \in 1 \dots r$ . Hence

$$\dots \leq \epsilon^{\lfloor \gamma/r \rfloor} \exp(\|\mathcal{L}\|) + \sum_{m=r}^k \frac{\|\mathcal{L}\|^m}{(m-1)!}.$$

□

**Theorem B.16.** *Let  $(\Phi_m)_{m=1}^k$  be a family contractions on a Banach space for any  $k \in \mathbb{N}$  all having fixed point projector  $\mathcal{E}$ . Let  $\mathcal{L}$  be a bounded Lindbladian such that  $e^{-\mathcal{L}s}$  is contractive for all  $s \in \mathbb{R}^+$ . Let  $\gamma \in \mathbb{R}^+$  such that for any consecutive sequence  $\Phi_W = \Phi_{j_1}, \dots, \Phi_{j_{k/\gamma}}, \Phi_W \geq_{cp} (1 - \epsilon)\mathcal{E}$ . Assume  $\sqrt{\gamma} \geq \max\{e^2\|\mathcal{L}\|, 2\}$ . Then for  $t > 0$ ,*

$$\left\| \prod_{m=1}^k (\Phi_m \circ e^{-\mathcal{L}t/k}) - e^{-\mathcal{E}\mathcal{L}\mathcal{E}t} \mathcal{E} \right\| \leq k(F_{\|\mathcal{L}\|t/k}^{(2)} + F_{\|\mathcal{E}\mathcal{L}\mathcal{E}\|t/k}^{(2)}) + \frac{1}{\gamma} F_{t\|\mathcal{L}\|}^{(1)} + \epsilon^{\sqrt{\gamma}} + 3e^{-\sqrt{\gamma}}.$$



*Proof.* The Theorem follows from Lemmas B.13, B.14, and B.15 with appropriate parameters. For general convenience, note that

$$\sum_{m=r}^k \|\mathcal{L}\|/(m-1)! = \|\mathcal{L}\| \sum_{m=r-1}^{k-1} \|\mathcal{L}\|^m/m!. \quad (50)$$

Let  $\Delta_1$  denote the contribution from Lemma B.13. Under the assumptions of this Theorem,

$$\Delta_1 \leq kF_{\|\mathcal{L}\|t/k}^{(2)}.$$

Let  $\Delta_2$  denote the contribution from Lemma B.14 with  $\alpha(m) = 1/\gamma m$  and  $n = k$ . Using Equation (50),

$$\Delta_2 \leq \sum_{m=1}^k \|\mathcal{L}\|m\alpha(m)/(m-1)! = \|\mathcal{L}\| \sum_{m=0}^k \frac{\|\mathcal{L}\|^m}{\gamma m!} = \frac{1}{\gamma} F_{\|\mathcal{L}\|}^{(1)}.$$

Consider Lemma B.15 with  $r = \lfloor \sqrt{\gamma} \rfloor$ . Via Equation (50) and Robbins's precise form of Stirling's approximation [Rob55],  $m! \geq \sqrt{2\pi m}(m/e)^m$ . Hence

$$\sum_{m=r-1}^{k-1} \|\mathcal{L}\|^m/m! \leq \sum_{m=r-1}^{k-1} \frac{1}{\sqrt{2\pi m}} \left( \frac{e\|\mathcal{L}\|}{m} \right)^m \leq \frac{1}{2\pi} \left( \frac{e\|\mathcal{L}\|}{r-1} \right)^{r-1} \frac{r-1}{r-1-e\|\mathcal{L}\|},$$

since we can overestimate the sum by relacing  $k$  by  $\infty$ . As long as  $r > e\|\mathcal{L}\| + 1$ , the bound is non-trivial. For large  $r$ , this function decays faster than exponentially in  $r$ , and hence in  $\sqrt{\gamma}$ . Letting the contribution from Lemma B.15 be denoted  $\Delta_3$ ,

$$\Delta_3 \leq \epsilon^{\sqrt{\gamma}} + 3e^{-\sqrt{\gamma}}$$

as long as  $\sqrt{\gamma} \geq \max\{e^2 t \|\mathcal{L}\|, 2\}$ .

Finally, let  $\Delta_4$  denote the contribution from again applying Lemma B.13, this time to relate the term  $\sum_{m=0}^k (\mathcal{E}\mathcal{L}\mathcal{E})^m/k^m = (1 - \mathcal{E}\mathcal{L}\mathcal{E}/k)^k$  to the desired  $\exp(-\mathcal{E}\mathcal{L}\mathcal{E}/k)$ . We bound  $\Delta_4$  by  $\sum_{r=1}^k F_{\|\mathcal{E}\mathcal{L}\mathcal{E}\|t_r}^{(2)}$ .

The full bound of the Theorem is given by  $\sum_{r=1}^4 \Delta_r$ .  $\square$

**Corollary B.17.** *Let  $(\Phi_m)_{m=1}^k$  be a family contractions with shared fixed point projector  $\mathcal{E}$ . Let  $\gamma \in (0, 1)$  such that for any consecutive sequence  $\Phi_W = \Phi_{j_1}, \dots, \Phi_{j_k/\gamma}$ ,  $\Phi_W \geq_{cp} (1 - \epsilon)\mathcal{E}$ . Let  $\mathcal{L}$  be a bounded Lindbladian such that  $e^{-\mathcal{L}s}$  is contractive for all  $s \in \mathbb{R}^+$ , and  $\sqrt{\gamma k} \geq \max\{e^2 t \|\mathcal{L}\|, 2\}$ . Then for  $t > 0$ ,*

$$\left\| \prod_{m=1}^k (\Phi_m \circ e^{-\mathcal{L}t/k}) - e^{-\mathcal{E}\mathcal{L}\mathcal{E}t} \right\| \leq k(F_{\|\mathcal{L}\|t/k}^{(2)} + F_{\|\mathcal{E}\mathcal{L}\mathcal{E}\|t/k}^{(2)}) + \frac{1}{\gamma k} F_{t\|\mathcal{L}\|}^{(1)} + \epsilon^{\sqrt{\gamma k}} + 3e^{-\sqrt{\gamma k}}.$$

Corollary B.17 follows immediately from Theorem B.16 and appropriate choice of parameters.

**Corollary B.18.** *Let  $\mathcal{S}$  be a bounded Lindbladian with fixed point projector  $\mathcal{E}$  on a Banach space such that  $\exp(-t\mathcal{S}/\gamma) \geq_{cp} \mathcal{E}$  for some  $\gamma \in \mathbb{R}^+$ . Let  $\mathcal{L}$  be a bounded Lindbladian such that  $e^{-\mathcal{L}t}$  is*

also contractive for all  $t \in \mathbb{R}^+$ , and  $\sqrt{\gamma} \geq \max\{e^2 t \|\mathcal{L}\|, 2\}$ . Then for any  $t \in \mathbb{R}^+$ ,

$$\left\| e^{-(S+\mathcal{L})t} - e^{-\mathcal{E}\mathcal{L}\mathcal{E}t} \right\| \leq \frac{1}{\gamma} F_{t\|\mathcal{L}\|}^{(1)} + \epsilon\sqrt{\gamma} + 3e^{-\sqrt{\gamma}}.$$

*Proof.* Via Theorem B.16,

$$\left\| \left( e^{-St/k} e^{-\mathcal{L}t/k} \right)^k - e^{-\mathcal{E}\mathcal{L}\mathcal{E}t} \right\| \leq \sum_{m=1}^k \left( F_{\|\mathcal{L}\|t/k}^{(2)} + F_{\|\mathcal{E}\mathcal{L}\mathcal{E}\|t/k}^{(2)} \right) + \frac{1}{\gamma} F_{t\|\mathcal{L}\|}^{(1)} + \epsilon\sqrt{\gamma} + 3e^{-\sqrt{\gamma}}.$$

The Corollary then follows from the Kato-Suzuki-Trotter formula [Suz76] as  $k \rightarrow \infty$ .  $\square$

The key distinction between Corollary B.18 and the main Theorems of [BFN<sup>+</sup>19] is that instead of an explicit weighting factor in the exponential,  $\gamma$  describes the decay properties of the semigroup. It is through this difference that we related the Zeno-like dynamics to semigroup decay. We recall via the definition of CMLSI that for any input density  $\rho$  and time parameter  $t$ ,

$$D(\exp(-St)(\rho) \|\mathcal{E}(\rho)) \leq \exp(-\lambda t) D(\rho \|\mathcal{E}(\rho)).$$

Hence via Pinsker's inequality,

$$\frac{1}{2} \|\exp(-St) - \mathcal{E}\|_{\diamond} \leq \exp(-\lambda t/2) \sqrt{(\ln C_{cb}(\mathcal{E}))/2},$$

where  $C_{cb}(\mathcal{E})$  is the Pimsner-Popa index of the fixed point projection. Let  $c_{\mathcal{E}}$  be defined such that  $\exp(-St) \geq_{cp} (1 - \epsilon)\mathcal{E}$  for

$$\epsilon = c_{\mathcal{E}} \exp(-\lambda t/2) \sqrt{(\ln c)/2}. \quad (51)$$

Proofs that such a  $c_{\mathcal{E}}$  exists and concrete bounds on its value appear as [BJL<sup>+</sup>21, Lemma 41], or [LaR21, Proposition 2.11]. Hence  $\exp(-tS/\gamma) \geq_{cp} (1 - \epsilon)\mathcal{E}$  whenever  $\lambda t/2\gamma \geq \ln(c_{\mathcal{E}} \sqrt{(\ln C_{cb}(\mathcal{E}))/2}/\epsilon)$ , or equivalently,

$$\gamma \leq \lambda t/2 \ln(c_{\mathcal{E}} \sqrt{(\ln C_{cb}(\mathcal{E}))/2}/\epsilon).$$

For a discrete channel  $\Phi$ , we similarly have that  $\Phi^k \geq_{cp} (1 - \epsilon)\mathcal{E}$  with

$$\epsilon = c_{\mathcal{E}}(1 - \lambda)^k \sqrt{(\ln C_{cb}(\mathcal{E}))/2}.$$

The condition for  $\epsilon < 1$  is satisfied when

$$k \geq \frac{\ln \epsilon - \ln(c_{\mathcal{E}} \sqrt{(\ln C_{cb}(\mathcal{E}))/2})}{\ln(1 - \lambda)}.$$

For Corollary B.17, we would substitute  $\lceil 1/\gamma \rceil$  for  $k$  in the above Equation. We may also choose  $\epsilon = 1/e$  to simplify the form of noted bounds. We hereby obtain our main Theorem on Zeno-like effects:

**Theorem B.19.** *Let  $\mathcal{L}$  be a bounded Lindbladian such that  $e^{-\mathcal{L}t}$  is contractive for all  $t \in \mathbb{R}^+$ . Let  $c_{\mathcal{E}}$  be given by Equation (51).*

(1) Let  $\mathcal{S}$  be a bounded Lindbladian with fixed point projector  $\mathcal{E}$  on a Banach space with  $\lambda$ -CMLSI and fixed point projection  $\mathcal{E}$ . Fix

$$\gamma = \frac{\lambda t}{\ln(ec\mathcal{E}\sqrt{(\ln C_{cb}(\mathcal{E}))/2})},$$

and assume  $\sqrt{\gamma} \geq \max\{e^2 t \|\mathcal{L}\|, 2\}$ . Then for any  $t \in \mathbb{R}^+$ ,

$$\left\| e^{-(\mathcal{S}+\mathcal{L})t} - e^{-\mathcal{E}\mathcal{L}\mathcal{E}t}\mathcal{E} \right\| \leq \frac{1}{\gamma} F_{t\|\mathcal{L}\|}^{(1)} + 4e^{-\sqrt{\gamma}} = O\left(\frac{1}{\lambda}\right).$$

(2) Let  $(\Phi_m)_{m=1}^k$  be a family contractions with shared fixed point projector  $\mathcal{E}$ . Fix  $\gamma$  such that

$$\left\lfloor \frac{1}{\gamma} \right\rfloor \leq \frac{\ln \epsilon - \ln(c\mathcal{E}\sqrt{(\ln C_{cb}(\mathcal{E}))/2})}{\ln(1-\lambda)},$$

and assume  $\sqrt{\gamma} \geq \max\{e^2 t \|\mathcal{L}\|, 2\}$ . Assume that for any consecutive sequence  $\Phi_W = \Phi_{j_1}, \dots, \Phi_{j_{k/\gamma}}$ ,  $\Phi_W \geq_{cp} (1-\epsilon)\mathcal{E}$ . Then

$$\left\| \prod_{m=1}^k (\Phi_m \circ e^{-\mathcal{L}t/k}) - e^{-\mathcal{E}\mathcal{L}\mathcal{E}t}\mathcal{E} \right\| \leq k(F_{\|\mathcal{L}\|t/k}^{(2)} + F_{\|\mathcal{E}\mathcal{L}\mathcal{E}\|t/k}^{(2)}) + \frac{1}{\gamma k} F_{t\|\mathcal{L}\|}^{(1)} + 4e^{-\sqrt{\gamma k}} = O\left(\frac{1}{k}\right).$$

Though the conditions of Theorem B.19 might not always be satisfied, one can always multiply  $\mathcal{S}$  by a constant factor until they are reached. This multiplication is analogous to the formulation in [BFN<sup>+</sup>19], where the bound is in terms of an explicit such factor. In contrast, our bound also depends explicitly on other aspects of  $\mathcal{S}$ , which might include such components as the connectivity of an underlying model, effective temperature, etc.

**Remark B.20.** *In principle, we could extend Theorem B.19 to unequally spaced times, replacing  $t/k$  by  $t_m$  for  $m \in 1 \dots k$ . This would however greatly complicate the Theorem and its proof to obtain a bit of generality we will not use. Hence we leave this to future work should it be needed.*

## APPENDIX C. PROOFS OF ENTRPY DECAY BOUNDS

**C.1. Discrete Compositions of Channels.** In this Subsection, we use the shorthand  $R_j := R_{U_j}$  to denote rotation via unitary conjugation.

**Lemma C.1.** *Let  $(\Phi_j)_{j=1}^m$  and respective  $(\mathcal{E}_j)_{j=1}^m, (U_j)_{j=1}^m$  be families quantum channels satisfying equation (19), (complete)  $\lambda_j$ -decay for each  $j$ , and equation (18) for intersection fixed point projector  $\mathcal{E}$ . Then*

$$D(\Phi_m \dots \Phi_1(\rho) \| R_m \dots R_1 \mathcal{E}(\rho)) \leq D(\rho | \mathcal{E}(\rho)) - \sum_j \lambda_j D(\Phi_j \dots \Phi_1(\rho) | \mathcal{E}_{j+1} \Phi_j \dots \Phi_1(\rho)).$$

*Proof.* For any  $m \in \mathbb{N}$ , using the chain rule and assumed complete decay for  $\Phi_m$ ,

$$\begin{aligned} D(\Phi_m \dots \Phi_1(\rho) \| R_m \dots R_1 \mathcal{E}(\rho)) &= D(\Phi_m \Phi_{m-1} \dots \Phi_1(\rho) \| \mathcal{E}_m R_m \mathcal{E} R_{m-1} \dots R_1(\rho)) \\ &= D(\Phi_m \Phi_{m-1} \dots \Phi_1(\rho) \| \mathcal{E}_m R_m \Phi_{m-1} \dots \Phi_1(\rho)) + D(\mathcal{E}_m R_m \Phi_{m-1} \dots \Phi_1(\rho) \| R_m \mathcal{E}_m \mathcal{E} R_{m-1} \dots R_1(\rho)) \\ &\leq (1 - \lambda_m) D(\Phi_{m-1} \dots \Phi_1(\rho) \| \mathcal{E}_m \Phi_{m-1} \dots \Phi_1(\rho)) + D(\mathcal{E}_m \Phi_{m-1} \dots \Phi_1(\rho) \| \mathcal{E}_m \mathcal{E} (R_{m-1} \dots R_1 \rho)) \\ &= D(\Phi_{m-1} \dots \Phi_1(\rho) \| R_{m-1} \dots R_1 \mathcal{E}(\rho)) - \lambda_m D(\Phi_{m-1} \dots \Phi_1(\rho) \| \mathcal{E}_m \Phi_{m-1} \dots \Phi_1(\rho)). \end{aligned}$$

Iterating, we arrive at

$$D(\Phi_m \dots \Phi_1(\rho) \| R_m \dots R_1 \mathcal{E}(\rho)) \leq D(\rho \| \mathcal{E}(\rho)) - \sum_j \lambda_j D(\Phi_j \dots \Phi_1(\rho) \| \mathcal{E}_{j+1} \Phi_j \dots \Phi_1(\rho)),$$

completing the Lemma.  $\square$

Again using chain rule iteration,

**Corollary C.2.** For  $(\Phi_j)_{j=1}^m$ ,  $(\mathcal{E}_j)_{j=1}^m$ ,  $(U_j)_{j=1}^m$ , and  $\mathcal{E}$  as in Lemma C.1,

$$D(\Phi_m \dots \Phi_1(\rho) \| R_m \dots R_1 \mathcal{E}(\rho)) \leq D(\rho \| \mathcal{E}(\rho)) - \min_j \lambda_j D(\Phi_m \dots \Phi_1(\rho) \| \mathcal{E}_m R_m \dots \mathcal{E}_1 R_1(\rho)).$$

**Lemma C.3.** Let  $(\Phi_j)_{j=1}^m$  be a family of quantum channels respectively having complete  $\lambda_j$ -decay, and obeying Equations (18) and (19) for  $(\mathcal{E}_j)$ ,  $(U_j)$ , and  $\mathcal{E}$ . If for some  $(\alpha_j > 0)_{j=1}^m$ ,

$$\sum_j \alpha_j \lambda_j D(\rho \| \mathcal{E}_j(\rho)) \geq D(\rho \| \mathcal{E}(\rho))$$

for a given density  $\rho$ , then

$$D\left(\frac{1}{\alpha} \sum_{j \in 1 \dots m} \alpha_j \Phi_j(\rho) \left\| \frac{1}{\alpha} \sum_{j \in 1 \dots m} \alpha_j R_j \mathcal{E}(\rho)\right.\right) \leq (1 - 1/\alpha) D(\rho \| \mathcal{E}(\rho))$$

with  $\alpha = \sum_j \alpha_j$ .

*Proof.* By biconvexity of the relative entropy,

$$\alpha D\left(\frac{1}{\alpha} \sum_j \alpha_j \Phi_j(\rho) \left\| \frac{1}{\alpha} \sum_j \alpha_j R_j \mathcal{E}(\rho)\right.\right) \leq \sum_j \alpha_j D(\Phi_j(\rho) \| \mathcal{E} R_j(\rho)). \quad (52)$$

Via the chain rule,

$$D(\Phi_j(\rho) \| \mathcal{E} R_j(\rho)) = D(\Phi_j(\rho) \| \mathcal{E}_j R_j(\rho)) + D(\mathcal{E}_j R_j(\rho) \| \mathcal{E} R_j(\rho)).$$

Since we assumed decay for  $\Phi_j$  and using the chain rule again,

$$\begin{aligned} D(\Phi_j(\rho) \| \mathcal{E} R_j(\rho)) &\leq (1 - \lambda_j) D(R_j(\rho) \| \mathcal{E}_j R_j(\rho)) + D(\mathcal{E}_j R_j(\rho) \| \mathcal{E} R_j(\rho)) \\ &= D(\rho \| \mathcal{E}(\rho)) - \lambda_j D(\rho \| \mathcal{E}_j(\rho)). \end{aligned}$$

Returning to the sum and using the assumed quasi-factorization,

$$\sum_j \alpha_j D(\Phi_j(\rho) \| \mathcal{E} R_j(\rho)) \leq \alpha D(\rho \| \mathcal{E}(\rho)) - \sum_j \alpha_j \lambda_j D(\rho \| \mathcal{E}_j(\rho)) \leq (\alpha - 1) D(\rho \| \mathcal{E}(\rho)).$$

Returning to Equation (52) completes the Lemma.  $\square$

**Theorem C.4** (Technical Version of Theorem 3.7). Let  $\Phi_m, \dots, \Phi_1$  be a sequence of quantum channels with respective fixed point conditional expectations  $(\mathcal{E}_j)_{j=1}^m$  obeying Equation (19) for  $(U_j)_{j=1}^m$  and Equation (18) for conditional expectation  $\mathcal{E}$ . Assume that each  $\Phi_j$  has (complete)  $\lambda_j$ -decay. If

$$(1 - \zeta) R_m \dots R_1 \mathcal{E} \leq_{cp} R_m \mathcal{E}_m \dots R_1 \mathcal{E}_1 \leq_{cp} (1 + \zeta(c - 1)) R_m \dots R_1 \mathcal{E} \quad (53)$$

for constants  $c > 1$  and  $\zeta \in (0, 1)$ , then  $\Phi_m \circ \dots \circ \Phi_1$  has (complete)  $(\min_j \lambda_j)\beta_{c,\zeta}$ -decay with  $\beta_{c,\zeta}$  as in Equation (16).

Let  $\mu$  be a measure on finite sequences  $s = (s_1, s_2, \dots)$  of indices  $j = 1 \dots m$  each containing  $k_{s,j}$  copies of each  $j$ th conditional expectation such that

$$(1 - \zeta)\mathcal{E} \leq_{cp} \sum_{s \in S} \mu(s) \prod_{i \in 1 \dots |s|} \mathcal{E}_{s[i]} \leq_{cp} (1 + \zeta(c - 1))\mathcal{E}, \quad (54)$$

where  $s[i]$  denotes the  $i$ th index in  $s$  and  $|s|$  the length of  $s$ . Let  $k = \sum_{s \in S} \mu(s) \sum_j k_{s,j} / \lambda_j$  and  $\Phi = (1/k) \sum_{s \in S} \mu(s) \sum_{j \in 1 \dots m} (k_{s,j} / \lambda_j) \Phi_j$ . Then  $\Phi$  has (complete)  $\beta_{c,\zeta}/k$ -decay.

*Proof.* The first part of the Theorem follows immediately from Corollary C.2 and Equation (16).

For the second part, we use the iterated chain rule as in [LaR21, Lemma 3.3], which implies for any sequence  $s$  of indices  $1 \dots m$  containing  $k_{s,j}$  copies of each index  $j \in 1 \dots m$ ,

$$\sum_{j=1}^m k_{s,j} D(\rho \| \mathcal{E}_j(\rho)) \geq D(\rho \| \mathcal{E}_{s[|s|]} \dots \mathcal{E}_{s[1]}(\rho)),$$

Convexity of relative entropy allows averaging with respect to measure  $\mu$  such that

$$\sum_s \mu(s) \sum_{j=1}^m k_{s,j} D(\rho \| \mathcal{E}_j(\rho)) \geq D\left(\rho \left\| \sum_s \mu(s) \sum \mathcal{E}_{s[|s|]} \dots \mathcal{E}_{s[1]}(\rho)\right.\right).$$

Equation (16) then implies that

$$\sum_s \mu(s) \sum_{j=1}^m k_{s,j} D(\rho \| \mathcal{E}_j(\rho)) \geq \beta_{c,\zeta} D\left(\rho \left\| \sum_s \mu(s) \sum \mathcal{E}_{s[|s|]} \dots \mathcal{E}_{s[1]}(\rho)\right.\right),$$

a quasi-factorization inequality. This inequality would satisfy the assumptions of Lemma C.3, but because the  $D(\rho \| \mathcal{E}_j(\rho))$  terms are obtained in that Lemma with  $\lambda_j$  weights, we counter these weights by adjusting the values of  $k_j$ . Then we apply the Lemma to complete the Theorem.  $\square$

Theorem 3.7 claims that the condition of Equation (13) is always satisfied for some combination of parameters given a rotation-free family  $(\Phi_j)$ . This follows from [LaR21, Remark 1.10] and the logic of its proof: long enough sequences of conditional expectations eventually converge to their overall fixed point in finite dimension.

**C.2. Continuous Semigroups.** If the stochastic generator  $\mathcal{S}$  in Equation (2) commutes with the Hamiltonian  $H$ , then CMLSI of  $\mathcal{L}$  is at least that of  $\mathcal{S}$  (even if  $\mathcal{S}$  may not commute with  $H$ ).

**Proposition C.5.** *Let  $\mathcal{L}$  be a Lindbladian with  $\sigma$ -detailed balance and fixed point projector  $\mathcal{E}$ . Let  $\tilde{\mathcal{L}}$  be a Lindbladian that commutes with  $\mathcal{E}$ . If  $\mathcal{L}$  has  $\lambda$ -(C)MLSI, then  $\mathcal{L} + \tilde{\mathcal{L}}$  decays states to the projection given by  $\mathcal{E}$  as though having  $\lambda$ -CMLSI. If  $\Psi_1, \dots, \Psi_m$  are quantum channels that commute with  $\mathcal{E}$ , then*

$$D(\Psi_1 \Phi^{t_1} \Psi_2 \Phi^{t_2} \dots \Phi^{t_{m-1}} \Psi_m(\rho) \| \Psi_1 \dots \Psi_m \mathcal{E}(\rho)) \leq e^{-\lambda t} D(\rho \| \mathcal{E}(\rho))$$

for any  $t_1, \dots, t_{m-1} > 0$  such that  $t_1 + \dots + t_{m-1} = t$ .

As a technical subtlety,  $\tilde{\mathcal{L}}$  may decay to a smaller subspace than that given by  $\mathcal{E}$  at a slower rate, such as by applying noise to a subsystem untouched by  $\mathcal{L}$ . For this reason we say that the semigroup induces relative entropy to  $\mathcal{L}$ 's fixed point subspace as though it has  $\lambda$ -(C)MLSI. The semigroup given by  $\mathcal{L} + \tilde{\mathcal{L}}$  may not have  $\lambda$ -(C)MLSI to its ultimate fixed point subspace, though it necessarily does under the conditions of Proposition C.5 if  $\tilde{\mathcal{L}}$  is a Hamiltonian.

*Proof.* First, we prove the discrete case, in which channels  $\Psi_1, \dots, \Psi_m$  surround and intersperse with  $\exp(-\mathcal{L}t)$ . Via the data processing inequality,

$$D(\Psi_1 \Phi^{t_1} \dots \Phi^{t_{m-1}} \Psi_m(\rho) \| \Psi_1 \dots \Psi_m \mathcal{E}(\rho)) \leq D(\Phi^{t_1} \Psi_2 \dots \Phi^{t_{m-1}} \Psi_m(\rho) \| \Psi_2 \dots \Psi_m \mathcal{E}(\rho)) .$$

Then using assumed (C)MLSI,

$$\begin{aligned} D(\Phi^{t_1} \Psi_2 \dots \Phi^{t_{m-1}} \Psi_m(\rho) \| \Psi_2 \dots \Psi_m \mathcal{E}(\rho)) &= D(\Phi^{t_1} \Psi_2 \dots \Phi^{t_{m-1}} \Psi_m(\rho) \| \mathcal{E}(\Psi_2 \Phi^{t_1} \dots \Phi^{t_{m-1}} \Psi_m(\rho))) \\ &\leq (1 - \lambda(t-1)) D(\Psi_2 \dots \Phi^{t_{m-1}} \Psi_m(\rho) \| \mathcal{E}(\Psi_2 \Phi^{t_1} \dots \Phi^{t_{m-1}} \Psi_m(\rho))) . \end{aligned}$$

Iterating the inequality completes the discrete case. For the continuous case, replacing  $\Psi_1, \dots, \Psi_m$  by a Lindbladian  $\tilde{\mathcal{L}}$ , we apply the same argument with the Kato-Suzuki-Trotter expansion, stating for small time  $\tau$  and bounded Lindbladians of the form in Equation (2) that

$$\Phi^\tau(\rho) = \Phi_{\tilde{\mathcal{L}}}^\tau \tilde{\Phi}^\tau(\rho) + O(\tau^2),$$

where  $\tilde{\Phi}^\tau$  is generated by  $\tilde{\mathcal{L}}$  and  $\Phi_{\tilde{\mathcal{L}}}^\tau$  by  $\mathcal{L}$ . We then have

$$D(\Phi^t(\rho) \| \mathcal{E}(\tilde{\Phi}^t(\rho))) = D(\Phi^\tau \tilde{\Phi}^\tau \Phi^{t-\tau}(\rho) \| \mathcal{E} \tilde{\Phi}^\tau \tilde{\Phi}^{t-\tau}(\rho)) + O(\tau^2 \log \tau),$$

where the correction term follows from the continuity of relative entropy with respect to a subalgebraic restriction, [Win16, Lemma 7] and [GJL20b, Proposition 3.7]. Via assumed (C)MLSI and the data processing inequality for relative entropy, the above Equation leads to the conclusion that

$$D(\Phi^t(\rho) \| \tilde{\Phi}^t \mathcal{E}(\rho)) \leq e^{-\lambda t} D(\Phi^{t-\tau}(\rho) \| \tilde{\Phi}^{t-\tau} \mathcal{E}(\rho)) + O(\tau^2 \log \tau) .$$

Iterating completes the Remark as we take the limit  $\tau \rightarrow \infty$ , using the fact that CMLSI holds for tracially self-adjoint Lindbladians as shown in [GR21] and [GJL21].  $\square$

In general, CMLSI will not hold for semigroups of the form in Equation (2). We will however prove decay as in Theorem 3.6. We may extend Lemma C.1 to the continuous limit, replacing  $\mathcal{E}_j$  by  $\mathcal{E}_t = \text{Rot}_{-iHt} \circ \mathcal{E}_0 \circ \text{Rot}_{iHt}$  and  $\Phi_j$  by  $\Phi^t$  for a semigroup  $(\Phi^t)$  with Hamiltonian part  $H$ . Then

$$\lim_{\tau \rightarrow 0} \tau \sum_t \lambda D(\Phi_t \dots \Phi_0(\rho) | \mathcal{E}_{t+\tau} \Phi_t \dots \Phi_0(\rho)) = \lambda \int_0^t D(\Phi^s(\rho) | \mathcal{E}_0 \Phi^s(\rho)) ds . \quad (55)$$

A naive approach might try to extend Corollary C.2 to continuum. We note however that in Equation (55), the result would contain a factor of the infinitesimal  $\tau$ , ultimately approaching zero. In particular, a major technical underpinning of decay merging [LaR21],

$$D(\rho \| \mathcal{E}(\rho)) + D(\rho | \tilde{\mathcal{E}}(\omega)) \geq D(\rho \| \mathcal{E} \tilde{\mathcal{E}}(\omega)) , \quad (56)$$

approaches triviality when  $\mathcal{E} \approx \tilde{\mathcal{E}}$ . The first step in deriving this inequality is to apply data processing, taking  $D(\rho \| \tilde{\mathcal{E}}(\omega)) \rightarrow D(\mathcal{E}(\rho) \| \mathcal{E} \tilde{\mathcal{E}}(\omega))$ . One may expand via the chain rule, noting

that  $D(\rho\|\tilde{\mathcal{E}}(\omega)) = D(\rho\|\tilde{\mathcal{E}}(\rho)) + D(\tilde{\mathcal{E}}\rho\|\mathcal{E}(\omega))$ , where the first term is nearly eliminated in the data processing step when  $\mathcal{E} \approx \tilde{\mathcal{E}}$ . There is however no way to tighten this inequality for general densities even when  $\mathcal{E} \approx \tilde{\mathcal{E}}$ :

**Counterexample C.6.** *Assume*

$$D(\rho\|\mathcal{E}(\rho)) + D(\rho\|\tilde{\mathcal{E}}(\rho)) \geq aD(\rho\|\mathcal{E}\tilde{\mathcal{E}}(\rho)).$$

*Via the chain rule,*

$$D(\rho\|\tilde{\mathcal{E}}(\rho)) \geq (a-1)D(\rho\|\mathcal{E}(\rho)) + aD(\mathcal{E}(\rho)\|\mathcal{E}\tilde{\mathcal{E}}(\rho)).$$

*If  $\rho = \mathcal{E}(\rho)$ , but  $\rho \neq \mathcal{E}(\rho)$ , then*

$$0 \geq (a-1)D(\rho\|\mathcal{E}(\rho)) + aD(\mathcal{E}(\rho)\|\mathcal{E}\tilde{\mathcal{E}}(\rho)),$$

*which can hold only if  $a \leq 1$ . Since we know that  $a \geq 1$  by the original Lemma,  $a = 1$ . For this counterexample, we may take  $\mathcal{E}$  to be a pinch on the qubit Bloch sphere and  $\tilde{\mathcal{E}} = ad_{U(\tau)} \circ \mathcal{E} \circ ad_{U(\tau)}$  for some qubit unitary family  $U(t)$ .*

The barrier to a continuous version of C.2 is not purely a mathematical technicality. As per Theorem 3.3 and Equation (20),  $\lim_{\tau \rightarrow \infty} \mathcal{E}_t \mathcal{E}_{t-\tau} \dots \mathcal{E}_\tau \mathcal{E}_0$  is entropy-preserving, so there is no way for it to converge in general to a convex combination including  $\mathcal{E}$ . More broadly, Zeno dynamics imply that if we tune up the strength of the decay component relative to the Hamiltonian, there are at least some instances in which the overall decay rate begins to decrease toward zero. Counterexample C.6 highlights that if we take a pair of conditional expectations that are infinitesimally rotated with respect to each other, their composition looks more like the first-applied conditional expectation followed by a rotation than like a broader mixing process.

For a GNS self-adjoint Lindbladian, the strategy of [LaR21] is to reduce the problem of combining constituent Lindbladians to one of quasi-factorization, which estimates the relative entropy to an intersection fixed point conditional expectation in terms of the relative entropy with respect to constituents. As illustrated in Counterexamples 3.1 and 3.2, this approach often fails with time dependence, as early dynamics may not sufficiently represent later mixing processes.

**Theorem C.7** (Technical Version of Corollary 3.4). *Let  $\mathcal{L} = i[H, \cdot] + \mathcal{S}$  generate  $\Phi^t$ , where  $H$  is a Hamiltonian and  $\mathcal{S}$  a Lindbladian with GNS detailed balance and  $\lambda_0$ -CMLSI to fixed point projector  $\mathcal{E}_0$ . Let  $\mathcal{E}$  denote the overall fixed point projector and  $R_t$  any persistent rotation. Assume that the semigroup is defined on a von Neumann algebra with finite trace. Let  $c := \ln(ec_{\mathcal{E}}(\mathcal{E}_0)\sqrt{(\ln C_{cb}(\mathcal{E}_0))/2})$  with  $c_{\mathcal{E}}$  given by Equation (51) and  $C_{cb}$  denoting the Pimsner-Popa index. If there exists a  $t_0 > 0$  for which  $D(\Phi^t(\rho)\|\mathcal{E}(\rho)) \leq e^{-\lambda t} D(\rho\|\mathcal{E}(\rho))$  for all  $t > t_0$ , then for sufficiently large  $\lambda_0$ ,*

$$\lambda \leq -\frac{4e^2\|H\|_{\infty}}{\sqrt{\lambda_0}} \left( \ln \left( \|R_{\sqrt{\lambda_0}/2e^2\|H\|_{\infty}} \mathcal{E} - e^{-i\lambda_0[\mathcal{E}_0(H), \cdot]/2e^2\|H\|_{\infty}} \mathcal{E}_0 \|_{\diamond} \right. \right. \\ \left. \left. - \frac{4e^2\|H\|_{\infty} c F_{\sqrt{\lambda_0}/e^2}^{(1)}}{\lambda_0^{3/2}} \right) - \ln(\sqrt{2 \ln C_{cb}(\mathcal{E})}) \right).$$

*Proof.* Let  $R_t\mathcal{E}$  denote the overall fixed point projector with possible rotation. By the assumption of CMLSI and Pinsker's inequality,

$$\|\Phi^t - R_t\mathcal{E}\|_\diamond \leq \sup_\rho \sqrt{2D(\Phi^t(\rho)\|R_t\mathcal{E}(\rho))} \leq e^{-\lambda t/2} \sqrt{2 \ln C_{cb}(\mathcal{E})}.$$

Via the triangle inequality,

$$\|\Phi^t - R_t\mathcal{E}\|_\diamond \geq \|R_t\mathcal{E} - e^{-it[\mathcal{E}_0(H), \cdot]} \mathcal{E}_0\|_\diamond - \left\| \Phi^t - e^{-it[\mathcal{E}_0(H), \cdot]} \mathcal{E}_0 \right\|_\diamond.$$

Via Theorem B.19 and with  $\lambda_0$  sufficiently large,

$$\left\| \Phi^t - e^{-it[\mathcal{E}_0(H), \cdot]} \mathcal{E}_0 \right\|_\diamond \leq \frac{2c}{\lambda_0 t} F_{2t\|H\|_\infty}^{(1)}.$$

Hence

$$e^{-\lambda t/2} \sqrt{2 \ln C_{cb}(\mathcal{E})} \geq \|R_t\mathcal{E} - e^{-it[\mathcal{E}_0(H), \cdot]} \mathcal{E}_0\|_\diamond - \frac{2c}{\lambda_0 t} F_{2t\|H\|_\infty}^{(1)}.$$

The bound is non-trivial only when

$$\lambda_0 t > \frac{\|R_t\mathcal{E} - e^{-it[\mathcal{E}_0(H), \cdot]} \mathcal{E}_0\|_\diamond}{2c F_{2t\|H\|_\infty}^{(1)}},$$

Solving for  $\lambda$ ,

$$\lambda \leq -\frac{2}{t} \left( \ln \left( \|R_t\mathcal{E} - e^{-it[\mathcal{E}_0(H), \cdot]} \mathcal{E}_0\|_\diamond - \frac{2c F_{2t\|H\|_\infty}^{(1)}}{\lambda_0 t} \right) - \ln(\sqrt{2 \ln C_{cb}(\mathcal{E})}) \right).$$

At first glance, it may appear that for extremely large  $t$ , this bound becomes arbitrarily small. Theorem B.19 requires, however, that  $\lambda_0 \geq \max\{4e^4 t^2 \|H\|_\infty^2, 4/t\}$ . We choose  $t = \sqrt{\lambda_0}/2e^2 \|H\|_\infty$  (which is valid as long as  $t$  and  $\lambda_0$  are both sufficiently large), eliminating  $t$  as a variable in the expression and completing the Theorem.  $\square$

The continuous structure of Lindbladian-driven decay nonetheless lets us to transform Equation (55) into a quasi-factorization inequality. We now prove a converse to CMLSI:

**Theorem C.8** (Restatement of Theorem 3.5). *Let  $(\Phi^t : t \in \mathbb{R}^+)$  be a continuous quantum Markov semigroup in the form of Equation (2) with stochastic generator  $\mathcal{S}$  having fixed point conditional expectation  $\mathcal{E}_0$ . Then*

$$D(\Phi^t(\rho)\|\mathcal{E}_0\Phi^t(\rho)) \geq \exp(-c\|\mathcal{S}\|_\diamond t/2) D(\rho\|\mathcal{E}_t(\rho)),$$

where  $c$  is the Pimsner-Popa index of the range of  $\mathcal{E}_0$  in its domain, and  $\mathcal{E}_t = R_{\exp(-iHt)} \mathcal{E}_0 R_{\exp(iHt)}$ .

*Proof.* We may write  $\mathcal{S}(\rho)$  as a sum of positive and negative parts for each input density  $\rho$ . Here  $\mathcal{S}(\rho) = \mathcal{S}_+(\rho) - \mathcal{S}_-(\rho)$ , where  $\mathcal{S}_+(\rho), \mathcal{S}_-(\rho) \geq 0$ . Since  $\text{tr}(\mathcal{S}(\rho)) = 0$ ,  $\text{tr}(\mathcal{S}_+(\rho)) = \text{tr}(\mathcal{S}_-(\rho))$  for all  $\rho$ . Hence  $\text{tr}(\mathcal{S}_+(\rho)) = (\text{tr}(\mathcal{S}_-(\rho)) + \text{tr}(\mathcal{S}_+(\rho)))/2 \leq \|\mathcal{S}\|_\diamond/2$ , and  $\|\mathcal{S}_+\|_\diamond \leq \|\mathcal{S}\|_\diamond/2$ . Since  $\mathcal{S}_+(\rho) \geq 0$ ,  $\mathcal{S}_+(\rho)/\alpha$  is a normalized density matrix for any  $\rho$  with some  $0 \leq \alpha \leq \|\mathcal{S}_+\|_\diamond$ .

For  $r > 0$  and any density  $\omega$ , let  $\tilde{\mathcal{S}}_\rho(\omega) := c(\|\mathcal{S}\|_\diamond/2)(\omega - \mathcal{E}_r(\mathcal{S}_+(\rho)/\alpha))$ . We know that  $\tilde{\mathcal{S}}_\rho$  is a valid Lindbladian, because it has the form of a convex state replacement. Then

$$-(\mathcal{S} + \tilde{\mathcal{S}}_\rho)(\rho) = \mathcal{S}^-(\rho) - \mathcal{S}^+(\rho) + c(\|\mathcal{S}\|_\diamond/2)\mathcal{E}_r(\mathcal{S}_+(\rho)/\alpha) - c(\|\mathcal{S}\|_\diamond/2)\rho \geq -(c\|\mathcal{S}\|_\diamond/2)\rho.$$



For asymptotically small  $\tau > 0$ ,

$$\exp(-\tau(\mathcal{S} + \tilde{\mathcal{S}}_\rho))(\omega) \geq (1 - \tau c \|\mathcal{S}\|_\diamond / 2)\omega - O(\tau^2).$$

Using the data processing inequality for relative entropy, for any  $t, r > 0$ ,

$$D(\Phi_t(\rho) \| \mathcal{E}_r \Phi_t(\rho)) \geq D(\exp(-\tau \tilde{\mathcal{S}}_{\Phi_{t-\tau}(\rho)}) \Phi^t(\rho) \| \exp(-\tau \tilde{\mathcal{S}}_{\Phi_{t-\tau}(\rho)}) \mathcal{E}_r \Phi^t(\rho)).$$

One can easily check that  $[\tilde{\mathcal{S}}_\rho, \mathcal{E}_r] = 0$ , so we can move  $\exp(-\tau \tilde{\mathcal{S}}_{\Phi_{t-\tau}(\rho)})$  past  $\mathcal{E}_r$  in the second argument to relative entropy. Using the Kato-Suzuki-Trotter formula,

$$\begin{aligned} \exp(-\tau \tilde{\mathcal{S}}_{\Phi_{t-\tau}(\rho)}) \Phi^t(\rho) &= \exp(-\tau(\mathcal{S} + \tilde{\mathcal{S}}_{\Phi_{t-\tau}(\rho)})) \mathcal{R}_{-iH\tau} \Phi^{t-\tau}(\rho) + O(\tau^2) \\ &\geq (1 - \tau c \|\mathcal{S}\|_\diamond / 2) \Phi^{t-\tau}(\rho) + O(\tau^2). \end{aligned} \quad (57)$$

Hence using the convexity of relative entropy and continuity of subalgebra-relative entropy,

$$\begin{aligned} D(\Phi_t(\rho) \| \mathcal{E}_0 \Phi_t(\rho)) &\geq (1 - \tau c \|\mathcal{S}\|_\diamond / 2) D(\mathcal{R}_{-iH\tau} \Phi_{t-\tau}(\rho) \| \mathcal{E}_r \mathcal{R}_{-iH\tau} \Phi_{t-\tau}(\rho)) + O(\tau^2 \ln \tau) \\ &= (1 - \tau c \|\mathcal{S}\|_\diamond / 2) D(\Phi_{t-\tau}(\rho) \| \mathcal{E}_{r+\tau} \Phi_{t-\tau}(\rho)) + O(\tau^2 \ln \tau). \end{aligned} \quad (58)$$

To complete the Lemma, we iterate  $t/\tau$  times and take the limit as  $\tau \rightarrow 0$ .  $\square$

Returning to Equation (55),

$$\lambda \int_0^t D(\Phi^s(\rho) \| \mathcal{E}_0 \Phi^s(\rho)) ds \geq \lambda \int_0^t e^{-r \|\mathcal{S}\|_\diamond / 2} D(\rho \| \mathcal{E}_r(\rho)) dr. \quad (59)$$

Since the right hand side is an integral of relative entropies with respect to distinct conditional expectations, we may apply a quasi-factorization as in [LaR21].

**Lemma C.9** (Continuous Quasi-factorization). *Let  $\mathcal{G}$  be a compact set and  $\mu_1, \dots, \mu_m : \mathcal{G} \rightarrow [0, 1]$  a sequence of probability measures on  $\mathcal{G}$ . Let  $\mathcal{E}_g$  denotes a conditional expectation parameterized by  $g$  to subalgebra  $\mathcal{N}_g$ , such that  $\bigcap_{g \in \mathcal{G}} \mathcal{N}_g = \mathcal{N}$  with conditional expectation  $\mathcal{N}$ . Assume Riemann integrability and that*

$$(1 + \zeta(c - 1))\mathcal{E} \geq_{cp} \int \dots \int \mathcal{E}_{g_m} \dots \mathcal{E}_{g_1} d\mu_1(g_1) \dots d\mu_m(g_m) \geq_{cp} (1 - \zeta)\mathcal{E}.$$

Then

$$\sum_{j=1}^m \int D(\rho \| \mathcal{E}_g) d\mu_j(g) \geq \beta_{c,\zeta} D(\rho \| \mathcal{E}(\rho)).$$

*Proof.* The main trick is similar to the proof of quasi-factorization in [LaR21], using Equation (56) to obtain

$$D(\rho \| \mathcal{E}_g) d\mu_j(g) \geq \int \dots \int \mathcal{E}_{g_m} \dots \mathcal{E}_{g_1} d\mu_1(g_1) \dots d\mu_m(g_m) D(\rho \| \mathcal{E}_{g_m} \dots \mathcal{E}_{g_1}(\rho)).$$

This Lemma then follows from convexity of relative entropy and Equation (16).  $\square$

**Theorem C.10** (Technical Restatement of Theorem 3.6). *Let  $\mathcal{L}$  be a Lindbladian in the form of Equation (2) with stochastic generator  $\mathcal{S}$  and Hamiltonian  $H$ . Let  $\mathcal{E}_t := R_{\exp(-iHt)}\mathcal{E}_0R_{\exp(iHt)}$ . Let  $\mathcal{E}$  denote the invariant subspace under decay at all values of  $t$ . Assume that  $\mathcal{S}$  has  $\lambda$ -CMLSI and for given  $\tau \in \mathbb{R}^+$  that*

$$(1 + \zeta(c - 1))\mathcal{E} \geq_{cp} \int_0^\tau \dots \int_0^\tau \mathcal{E}_{t_m} \dots \mathcal{E}_{t_1} d\mu_1(t_1) \dots d\mu_m(t_m) \geq_{cp} (1 - \zeta)$$

where  $\mu_1, \dots, \mu_m : [0, \tau] \rightarrow [0, 1]$  are probability measures and  $\alpha > 0$  such that

$$\sum_{j=1}^m \int_0^\tau d_{\mu_j}(t) |t\rangle\langle t| \leq \alpha \int_0^\tau e^{-\frac{c_{cb}(\mathcal{E}_0)\|\mathcal{S}\|_{\diamond} t}{2}} |t\rangle\langle t| dt,$$

where  $|t\rangle\langle t|$  denotes a basis vector on the compact set  $[0, \tau]$ . Then  $\exp(-\mathcal{L}\tau)$  has  $\alpha\beta_{c,\zeta}\lambda$ -decay.

The condition are satisfied for any  $\tau > 0$  with some  $\alpha > 0$ ,  $\zeta \in (0, 1)$ , and  $c > 1$ .

*Proof of Theorem 3.6.* The first part of the proof is given by the extension of Lemma C.1 via Equation (55), from which we obtain that

$$D(\Phi^t(\rho) \| R_{\exp(-iHt)}\mathcal{E}(\rho)) \leq D(\rho \| \mathcal{E}(\rho)) - \gamma\lambda \int_0^t D(\Phi^r(\rho) \| \mathcal{E}_0\Phi^r(\rho)) dr.$$

From Theorem 3.5,

$$\int_0^t D(\Phi^r(\rho) \| \mathcal{E}_0\Phi^r(\rho)) dr \geq \int_0^t e^{-c\|\mathcal{S}\|_{\diamond} r} D(\rho \| \mathcal{E}_r(\rho)) dr.$$

Lemma C.9 for  $m$  copies of the above completes the quantitative part of the Theorem.

The existence of constants satisfying the conditions of the Theorem follows [LaR21, Remark 1.10], in which it was shown that within finite dimensions, a composition of conditional expectations to high enough power eventually reaches a convex combination involving the overall fixed point. Via the semigroup property, we know that the fixed point of  $\exp(-\tau\mathcal{L})$  is the same fixed point as for the entire semigroup.  $\square$

The above proof and Theorem 3.6 imply that for any  $\tau > 0$ ,  $\exp(-\tau\mathcal{L})$  shows some relative entropy decay with respect to the fixed point of the overall semigroup. Examining the primary argument in terms of continuous quasi-factorization, the set of conditional expectations  $\{\mathcal{E}_t : 0 \leq t \leq \tau\}$  suffices to obtain quasi-factorization, and a sequence of these conditional expectations ultimately decays to the overall fixed point. One may wonder if it is possible to extrapolate to  $\tau = 0$ , finding CMLSI after all. This fails not because there is some finite time lacking decay, but because the constant may approach zero too quickly in this limit. While  $\{\mathcal{E}_t : 0 \leq t \leq \tau\}$  contains enough conditional restrictions to reach the overall fixed point of the semigroup, it is not necessarily efficient. Indeed, at small  $\tau$ , the projectors are extremely close together and generally have a highly unfavorable quasi-factorization constant. Nonetheless, they contain enough information about the semigroup to fully distinguish its ultimate fixed point assuming one exists.

**C.3. Additional Examples.** We briefly include two examples to motivate certain preferences in the form of inequalities. First is a situation in which the rotation in  $\lambda$ -decay allows the inequality to remain meaningful where usual decay to a fixed point breaks down.

**Example C.11** (Effectively Classical Circuits). Let a sequence of channels  $\Phi_1, \dots, \Phi_m$  be constructed from the gate set  $\{Id, X, CX, TOFFOLI\}$  or another universal set for reversible classical computation. Let each such channel also impose strong dephasing noise in the computational basis on all of the qubits on which it acts. In this scenario, one would typically expect fast decay to the computational basis, enforcing classicality on deep circuits of this form. Technically, however, such a channel sequence never converges to an invariant subspace. If we take  $\mathcal{E}$  to be the projector to the fully dephased subspace, then  $D(\Phi_m \dots \Phi_1(\rho) \| \mathcal{E}(\rho))$  fails to converge and may even diverge toward infinity, because the effectively classical gates still induce non-trivial changes in the computational basis. The notion of  $\lambda$ -decay is more meaningful for this system. Since the conditional expectation to the fixed point algebra commutes with the noisy gates, calculating the decay rate for explicit sequences  $\Phi_m \dots \Phi_1$  should in many cases be fairly simple.

The second example illustrates a case in which the decay constant of a family of Lindbladians increases in strength, but not in such a way that one could directly compare them in the matrix ordering. Hence Theorem 3.3 implies constants not obvious from those of [BFN<sup>+</sup>19].

**Example C.12.** Let  $G$  be a finite, undirected graph on  $n$  vertices, defined as a set of pairs  $(i, j) : i, j \in 1 \dots n$ . Let

$$u_{i,j} = |i\rangle\langle j| + |j\rangle\langle i| + \sum_{r \neq i,j} |r\rangle\langle r|$$

represent a single edge on Hilbert space of dimension at least  $n$ , with the possibility of extension by an arbitrary auxiliary system with an interaction Hamiltonian  $H$ . As noted in [LaR21], the complete graph Lindbladian given by

$$\mathcal{S}_n(\rho) = \rho - \sum_{i,j \in 1 \dots n} |i\rangle\langle j|$$

has  $O(n)$ -CMLSI. Also noted therein is that  $C_{cb}(\mathcal{E}_0) \leq n^2$ . Hence via Theorem 3.3, the complete graph is  $O(\ln n/n)$  even though for  $\alpha > 1$ ,  $\mathcal{S}_{\alpha n} \geq a\mathcal{S}_n$  only up to  $a = 1$ . Accelerated convergence to the Zeno limit arises because the structure of all-to-all interactions, which in the absence of a  $1/n$  normalization factor cause the degree of the graph and hence the mixing time of a random walk to decrease with size.

#### APPENDIX D. EXPERIMENTAL DETAILS

Experiments were run on the *ibmq\_santiago* through Qiskit. To minimize shot noise, 32000 shots were used circuit. A single-qubit process tomography uses 12 circuits, each with a distinct combination of preparation and post-processing gates. Tomography circuits were generated automatically using Qiskit’s “process\_tomography\_circuits” subroutine and fit using Qiskit’s “ProcessTomographyFitter.” At the time of running, the two auxiliary qubits respectively had reset times of  $0.99\mu s$  and  $1.00\mu s$ . The auxiliary qubit had  $T_1$  of  $156\mu s$  and  $T_2$  of  $158\mu s$ . The  $CX$  gate

from  $A$  to  $B$  had reported error 0.0076, which one may interpret as one minus the fidelity as determined by IBM’s randomized benchmarking [MGE12]. Though the full  $CX$  gate would take  $256ns$ , the pulsed  $\Phi_{ZX}(\pi/(2k))$  was slightly shorter, taking  $214ns$  for its fully entangling version and  $155ns$  when  $k > 1$ . For larger values of  $k$ , smaller  $XZ$  rotations were applied by reducing the pulse amplitude using Qiskit’s `RZXCalibrationBuilder` based on techniques of [SBEP21]. The  $RZX$  form of interaction was chosen because of its relation to commonly used gates on this computing platform.

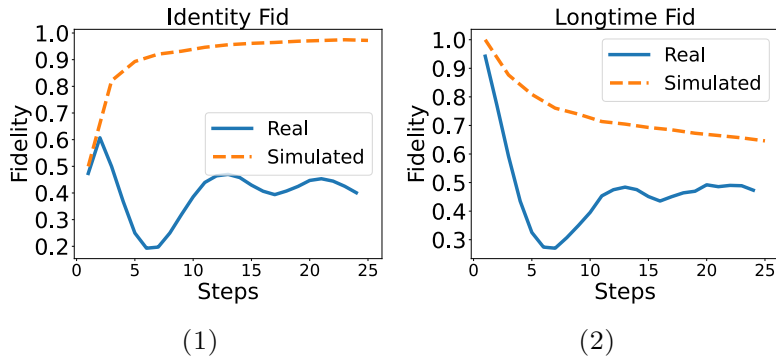


FIGURE 5. Plots of raw metrics for qubit  $B$  undergoing the channel described by Equation (5). (1) Fidelity of induced channel’s Choi matrix with the identity process. (2) Fidelity with the long-time fixed point.

Raw metrics are shown in Figure 5. To better represent and understand the actual channels observed, we use a similar method as the  $D^4$  model in [LSI<sup>+</sup>22]. While the intended decoherence is  $X$ -basis dephasing as inferred in Subsection 5.1, unintended decoherence commonly appears as a combination of depolarizing, amplitude damping, dephasing, and coherent phase drift. Unlike in [LSI<sup>+</sup>22], here we study single channels rather than repeated composition of the same channel, so we do not use the “ $t$ ” parameter considered therein. We make the simplifying assumption that noise is applied simultaneously as in a continuous semigroup - this does not constrain the parameter range of the model but resolves the ambiguity due to non-commutativity of amplitude damping with depolarizing noise and  $X$ -basis decoherence. We add continuous  $X$ -basis dephasing to the original model. We denote by  $\epsilon$  a depolarizing parameter, by  $\eta$  a  $Z$ -basis amplitude damping parameter, by  $\delta$  a  $Z$ -basis dephasing parameter, by  $\theta$  a phase drift angle, and by  $\chi$  the same  $X$ -basis dephasing parameter as in Equation (14).

A channel is fully characterized by its Choi matrix, the result of applying the channel to one half of a maximally entangled pair. The Choi matrix of an identity channel is given by the density matrix of  $(|00\rangle + |11\rangle)/\sqrt{2}$ , a maximally entangled state in which the output and reference mirror each other. To infer noise parameters from a Choi matrix, we solve for specific elements of the Choi matrix under modeled noise in the computational basis. In particular, letting  $M_{j,l}$

denote the  $j, l$ th entry,

$$M_{11} = \left( \frac{1}{2} - \frac{\epsilon + 2\eta + \chi}{4(\epsilon + \eta + \chi)} \right) e^{-(\epsilon + \eta + \chi)} + \frac{\epsilon + 2\eta + \chi}{4(\epsilon + \eta + \chi)}, \text{ and}$$

$$M_{44} = \left( \frac{1}{2} - \frac{\epsilon + \chi}{4(\epsilon + \eta + \chi)} \right) e^{-(\epsilon + \eta + \chi)} + \frac{\epsilon + \chi}{4(\epsilon + \eta + \chi)}.$$

Because the channel only touches one half of the Bell pair, we may assume that  $M_{22} = 1/2 - M_{11}$  and that  $M_{33} = 1/2 - M_{44}$ . For off-diagonal elements,

$$\begin{aligned} |M_{14}| + |M_{23}| &= \frac{1}{2} e^{-(\eta/2 + \epsilon + \delta)} \\ |M_{14}| - |M_{23}| &= \frac{1}{2} e^{-(\eta/2 + \epsilon + \delta + \chi)}. \end{aligned} \quad (60)$$

These 4 matrix elements suffice to fully define the 4 parameters  $\epsilon, \eta, \delta$ , and  $\chi$ . In practice, we find simple a simple formula for  $\chi$  as in (14), which allows us to extract this parameter immediately. We then use Scipy's "scipy.optimize.minimize" subroutine to solve for  $\epsilon$  and  $\eta$ , after which we can easily solve for  $\delta$  in terms of  $|M_{14}| + |M_{23}|$ . We find  $\theta$  independently as the phase of  $M_{14}$ . These inferred parameters uniquely determine  $M_{11}, M_{22}, M_{12}, M_{14}, M_{23}, M_{41}, M_{32}, M_{33}$ , and  $M_{44}$ . In this model, we assume that other elements are zero.

Figure 6 shows unintended noise parameters over time. While coherent phase drift is non-

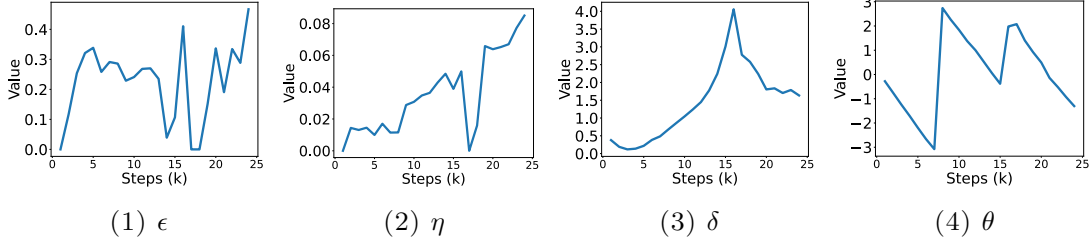


FIGURE 6. Plots of noise parameters by step number.

trivial, this should not have a substantial effect on inferred  $X$ -basis dephasing. Otherwise, the dominant noise contribution is from  $Z$ -basis dephasing, which by reducing the magnitude of off-diagonal elements may reduce the precision of the inferred  $\chi$  in Equation (14). Dominance of  $Z$ -basis dephasing as unintended noise is consistent with passive decoherence during resets, but this explanation is not consistent with the similarity in reported  $T_1$  and  $T_2$  noise and lack of substantial amplitude damping contribution. Dephasing noise appears to peak at 16 steps, the same point where  $\chi$  becomes negative (and is set to 0 in further parameter inference), while other parameters show spikes at this point. This observation is consistent with the explanation that  $\chi$  becomes negative due to uncertainty in the ratio of the sum and difference in Equation (60) when both have small values. It also appears that the pulsed interactions might drive dephasing noise or suppress other kinds of noise.

A qubit undergoing dephasing noise in two bases also is effectively depolarized. Though complete depolarization is indistinguishable from complete dephasing in both of two mutually

unbiased bases, the partial versions of these channels do allow one to distinguish noise contributions via the ratio of each dephased contribution to the depolarized portion. In Figure 6, the depolarizing parameter corresponds to that left over after accounting for both kinds of dephasing. Here we see evidence that in this case, depolarizing noise arises more as a consequence of dephasing in two bases than via direct replacement of the state by complete mixture.

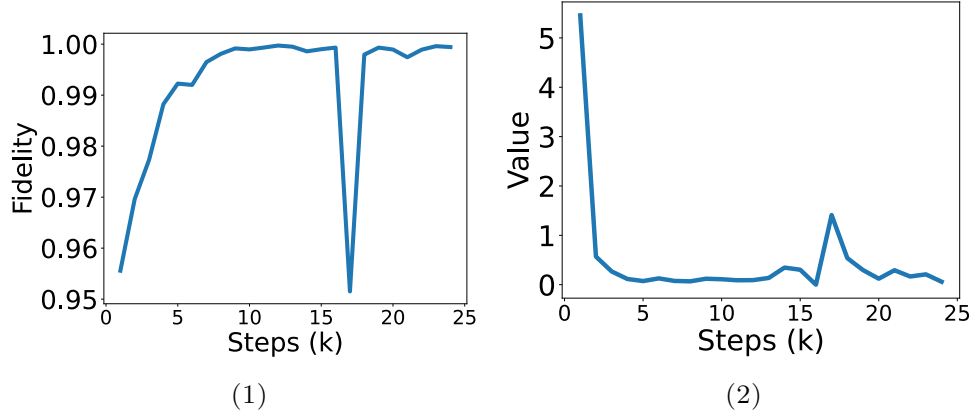


FIGURE 7. (1) Process fidelity of inferred model's reconstructed channel with the observed channel. (2) Inferred dephasing parameter  $\chi$  as in Equation (14).

Finally, we arrive at the culmination of this analysis in Figure 7. First, Figure 7.(1) shows the process fidelity of the inferred model with the channel tomography. Since observed fidelities are at least 95% with a mean of 99%, the noise model does not lose much information about the state. Figure 7.(2) shows the inferred  $\chi$  parameter, which is used to reconstruct the cleaned data for Figure 3.

UNIVERSITY OF CHICAGO, CHICAGO, IL 60637, USA  
*Email address*, Nicholas LaRacunte: [nlaracunte@uchicago.edu](mailto:nlaracunte@uchicago.edu)